Lawrence Berkeley National Laboratory
Recent Work

Title

Alumina-Silicon Carbide Composites from Coated Powders

Permalink

https://escholarship.org/uc/item/3244898w

Author

Mitchell, T.D.

Publication Date

1990-12-01

Lawrence Berkeley Laboratory
UNIVERSITY OF CALIFORNIA

Materials & Chemical Sciences Division

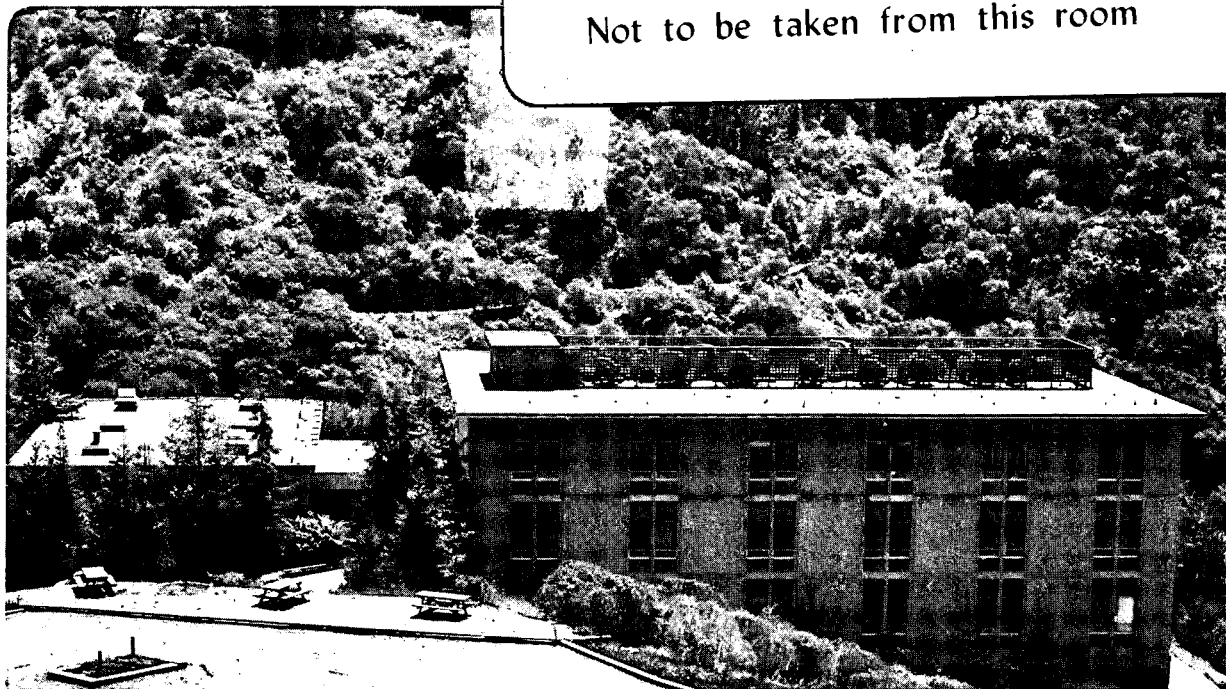## Alumina-Silicon Carbide Composites from Coated Powders

T.D. Mitchell, Jr.
(M.S. Thesis)

December 1990

DISCLAIMER

Alumina-Silicon Carbide Composites

from Coated Powders

Tyrone D. Mitchell, Jr.

M.S. Thesis

Department of Materials Science & Engineering
University of California, Berkeley
and
Materials Sciences Division
Lawrence Berkeley Laboratory
Berkeley, CA 94720
12/90

Table of Contents

Acknowledgements

I would like to thank everyone who helped with the information and structure of the work that went into this document. I specifically want to acknowledge my advisor, Lutgard C. De Jonghe, for his guidance and advice during this work. Special thanks, of course , go to my parents, without whom I would not be where I am today.

Alumina-Silicon Carbide Composites
from Coated Powders

by

Tyrone D. Mitchell, Jr.

Abstract

Previous technology for alumina coating of silicon carbide whiskers was applied to silicon carbide platelets. Process parameters were developed to ensure successful coating of platelets and to produce composites of varying final platelet volume fractions. Coated whisker composites were hot pressed to near full density or pressureless sintered to closed porosity despite high whisker loading. In some cases, pressureless sintering resulted in near full density with high (30 volume percent) whisker loading. Coated platelet composites were hot pressed to near full density and pressureless sintered to closed porosity with high loading (35 vol%). Mechanical properties of these composites were evaluated, including fracture toughness and bend strength.

1. Introduction

1.1 Goals

Despite excellent wear, corrosion and temperature resistance, structural applications of ceramic materials are limited by their brittleness. Ceramic-ceramic composites (most notably reinforcement of a ceramic matrix with ceramic whiskers) are of great interest because of their improved strength and fracture toughness. Significant improvement in mechanical properties is obtained upon addition of large volume fractions of a reinforcing phase. In particular, several studies of the Al_2O_3 - SiC whisker system show fracture toughness increasing with whisker volume fraction [1-3].

The improvement in mechanical properties upon introduction of a second phase is at least partially offset by greater difficulties in processing. The reinforcing particles tend to cluster together to form "networks" that hinder densification of the microcomposite [3,4]. Lange et al. [4] have described two mechanisms by which this hindrance to densification may occur. These are: 1) extra deformation of the matrix is necessary due to the excluded volume inside these network clusters; and 2) continuous touching networks support the stress associated with densification.

Each of these mechanisms can be related to the inability to pressureless sinter microcomposites with high volume fractions (>20%) of reinforcing phase to closed porosity. In the first mechanism, the matrix is required to sinter into areas kept devoid of matrix particles by the bulk volume of the reinforcing clusters. A

large external load, as used when hot pressing, can break the clusters and force in matrix material. In pressureless sintering, however, no external load exists to break the clusters and the excluded volume remains. In the second mechanism, parts of the matrix are shielded from the densification stress by load-bearing networks. Again a large external load can surpass the stress-bearing capability of the networks, but in pressureless sintering the sintering stress alone is not great enough to accomplish this and the voids remain.

These conclusions have been supported by previous work in the free sintering of Al_2O_3 - SiC whisker composites. Tiegs and Becher [3] obtained very dense composites (greater than 95% of theoretical) by pressureless sintering with 10 volume% whiskers, but higher volume fractions yielded correspondingly lower densities. Thus, despite its commercial attractiveness, pressureless sintering to closed porosity has to this point been difficult and, with high volume fractions of reinforcement, unobtainable.

Producing a composite with a homogeneously distributed second phase is also a problem. Poor distribution due to agglomeration can cause matrix-rich areas free of reinforcing particles, lowering gains in strength and toughness. For example, a progressing crack can wind through weak matrix regions and effectively avoid energy dissipative contact with the reinforcing particles.

Ideally, the green microstructure of a microcomposite would have each reinforcing particle encapsulated in enough matrix material to prevent contact during densification. This microstructure can be achieved by introducing the matrix phase as a coating on individual second phase particles to produce a "coated powder." Coated

powders greatly reduce or eliminate second phase particle contacts, enabling a more homogeneous phase distribution. Coated powders are also more easily densified which allows processing under more mild conditions.

1.2 Coating Process Review

The coating process used in this work was developed by Kapolnek and De Jonghe [5], in which an alumina precursor was precipitated onto the surface of SiC whiskers. The background for developing this process, though described in detail in Ref. [6], will be summarized here as it will later be applied to SiC platelets.

The process of coating a core particle with a ceramic precursor consists of nucleation and growth of the matrix phase (from solution) on the surface of the core particle. Precipitation of ceramic precursors has been investigated, specifically the homogeneous precipitation of nearly spherical powders[7-14]. Alumina particles have been produced in this manner through several chemical methods[15]. One method that has been particularly successful involves hydrolyzing aluminum sulfate in an aqueous solution. A solution of urea and aluminum sulfate is heated to sufficient temperature to decompose the urea (90 to 100°C), which in turn releases ammonium and hydroxide ions into solution through the reaction: $(H_2N)2CO + H_2O + 2H_3O^+ \rightarrow CO_2 + 2H_2O + 2NH_4^+$ [16]. The introduction of hydroxide ions increases the pH of the solution [15], which then causes hydrolysis of the aluminum cations to species with lower solubility[17]. The product, hydrated basic aluminum sulfate (HBAS), may then exceed its solubility limit by an amount large

3

enough to allow homogeneous nucleation. Precipitation of HBAS nuclei lowers the concentration of dissolved Al(III), causing the HBAS concentration to drop below the limit for homogeneous nucleation. The existing nuclei will continue to grow, however, until the concentration of HBAS drops below the solubility limit, ending the process. HBAS can then be thermally decomposed to form Al_2O_3. This method was studied and developed in refs. [15,16,18,19], and the work by Kapolnek & De Jonghe is based on ref. [15].

Kapolnek & De Jonghe modified the process described in [15] to produce SiC whiskers with thick alumina coatings. SiC whiskers were added to the aluminum sulfate - urea solution prior to heating. As before, the urea decomposition caused the pH to increase and the Al(III) concentration to exceed its solubility limit. However, before HBAS precipitated homogeneously it was removed from solution by the energetically more favorable heterogeneous precipitation onto the surface of the SiC whiskers. With a slow pH increase, the HBAS precipitation removed enough Al(III) ions to completely prevent homogeneous precipitation. Rigid temperature control was necessary to control the rate of urea decomposition and, correspondingly, the rate of the pH rise[6]. This became even more important in the coating of platelets, as will be shown later. A modified LaMer diagram describing this process is shown in figure 1.

2. Experimental Procedure

2.1 Coating of SiC Platelets

Coated SiC platelets were produced in much the same manner as coated SiC whiskers, but with a few modifications to the process of Kapolnek & De Jonghe. A small amount of polymeric dispersant was dissolved at room temperature in distilled water prior to the addition of the C-Axis Technologies SiC platelets. This solution was thoroughly dispersed with an ultrasonic probe for several minutes to remove any agglomerates. The dispersed platelets were then added to a solution containing aluminum sulfate hydrate and urea that had been dissolved in distilled water inside a flat bottomed boiling flask. The concentrations of the species in solution were 0.1M aluminum sulfate hydrate, 12 g/l urea, 10 g/l SiC platelets, and 0.7 g/l dispersant.

The boiling flask was then partially immersed in an oil bath resting on a magnetic stirring hot plate. A water-cooled condenser tube was placed over the mouth of the flask to prevent excessive water evaporation during heating. The solution was vigorously stirred as the temperature was slowly increased over a period of a few hours to a final temperature of 90 to 92°C and maintained at that temperature for approximately 22 hours. The solution was then cooled and allowed to settle.

After the supernatant was discarded, the remaining solids were rinsed with distilled water followed by two acetone washes to remove the water. Air drying then produced a fluffy, flowing coated powder. This powder was then calcined in air at 850°C overnight to

convert the coatings to alumina. Care was taken not to calcine the powder any longer than necessary to prevent formation of SiO_2 on the SiC surface by oxidation. X -ray diffraction experiments performed on pre and post - calcined coated platelet powders showed the coatings to be HBAS before calcining and crystalline alumina after calcining.

2.2 Densification of Coated Powders

2.2.1 Hot Pressing

The alumina-coated SiC whisker or platelet powder was loaded directly into a graphite die. The sample was heated at 20°C per minute to a final temperature of 1600°C, where it was held for 1 hour under an applied load of 35 MPa (5000 psi). Hot pressed discs were diamond polished to 1μm for observation using an optical microscope or SEM, or sectioned for mechanical property testing.

2.2.2 Pressureless Sintering

Pressureless sintering was performed with the addition of 2.0 wt.% Y_2O_3 and 0.5 wt.% MgO as sintering aids [3]. The coated powder and additives were dispersed in acetone with an ultrasonic probe and air dried. The dried powder was then uniaxially pressed into compacts at 21 Mpa (3000 psi) before isostatic pressing at 840 MPa (120,000 psi).

The compacts were sintered in a graphite element furnace under an atmosphere of flowing He gas at a temperature of 1850°C for 30 minutes. The compacts were packed in a blend of Al_2O_3 and SiC

powder in a closed SiC or Al_2O_3 crucible to prevent a reaction between the Al_2O_3 in the sample and the graphite in the furnace. Densities were determined after densification by Archimedes' method, with glycerol used as the reference liquid. Sintered bars were diamond polished to 1μm for SEM and optical microscope observation, or sectioned for mechanical property testing.

2.3 Mechanical Property Testing

Bend strength and fracture toughness of the coated powder composites were measured in four point bending on bars 2.0mm x 2.0mm x 25mm dimensions on a jig with a 6.4mm inner span and a 19mm outer span. After sectioning, some bars were indented on the tensile surface with a 150N Knoop indent such that the long axis of the indent was perpendicular to the applied stress axis. This indent created an elliptical flaw with a radius of 250mm to 300mm (figure 2). All bend bars were surface polished to 6μm and the tensile edges bevelled to remove stress concentrations and any large edge flaws inflicted during sectioning.

Bend strength was determined under a crosshead speed of 0.5mm/sec from the relation [20]:

$$\sigma = (3Pa) / (bh^2) \qquad (1)$$

Where σ is the stress at fracture, P the maximum force, a is 1/2 the distance between the outer and inner spans, b the bar width, and h the bar thickness.

On indented bars, the fracture toughness was determined from the relation[21]:

$$K_{1C} = (2/\sqrt{\pi})\sigma(\sqrt{a})$$ (2)

where K_{1C} is the critical stress intensity factor (toughness), a the initial flaw radius, and σ the stress determined from equation (1).

3. Results and Discussion

3.1 Production of Coated SiC Platelets

3.1.1 Production of Coated Powders by Precipitation for Solution

Successful precipitation of coatings onto powders from solution requires control of several variables to produce the desired interaction between a particulate suspension A and the material that is to be precipitated out of solution, B [23]. Possible results of such A-B experiments are:

(1)   B precipitates homogeneously out of solution, creating particles of B which do not interact with A. The result is a mix of discrete A and B particles, undesirable in this case.

(2)   B precipitates homogeneously and eventually agglomerates with particles of A. This heterocoagulation would produce large nonuniform clumps of an A-B amalgam, also undesirable.

(3)　B precipitates homogeneously, and at a very early stage small B nuclei flocculate onto particles of A. The nuclei then grow on the A surface, producing a B coating on the A particle. This result is more desirable than (2) above, as long as the B particles are very small compared to the A particles.

(4)　B precipitates heterogeneously on the A surface, producing a uniform coating which becomes thicker as nucleation and growth continue. This is probably the most desirable interaction, and in order to produce coated powders in this manner the following requirements are proposed [23].

3.1.1.1 Separation of Nucleation and Growth

Figure 3 is a LaMer diagram desribing the variation of solute concentration with time for the solution precipitation process. Curve 'a' represents homogeneous nucleation, curve 'b' a combination of homogeneous and heterogeneous nucleation, and curve 'c' pure heterogeneous nucleation.

Heterogeneous precipitation begins when the concentration of solute, in this case a reaction product, reaches C^*_{hetero}. For optimal results, this should occur without surpassing the homogeneous nucleation limit, albeit only for a brief time (curve 'b'). The most desirable case is curve 'c', in which only heterogeneous nucleation occurs before entrance into the growth regime.

3.1.1.2 Dispersion Stability

To obtain well dispersed coated powders, a stable dispersion is important during nucleation and growth. Formation of agglomerates prior to precipitation could result in the formation of large coated particle clumps, so care must be taken to ensure a well dispersed solution (most likely through vigorous stirring).

3.1.1.3 Effect of the Core Particle Surface Area

The surface area of the core particle must be sufficient to allow the reactants to be removed from solution at a rate such that the solute concentration never reaches C^*_{homo}. If this occurs for even a brief time (curve 'b'), the result will be a mix of coated particles and free precipitates. The appropriate surface area of the core particles is therefore related to the rate of generation of the reaction products, r_g, and the rate of removal of these products by precipitation, r_r. The minimum surface area available for precipitation, A_{min}, controls the maximum allowable concentration of the reaction products before the onset of homogeneous nucleation, C_{max}. Thus, for a given generation rate r_g, A_{min} is defined by the equation [23]:

$$r_g = k A_{min} (C^*_{homo} - C_s)\qquad(3)$$

where k is a constant, $C_{max} = C^*_{homo}$ and C_s is the concentration of reaction products at the solubility limit.

There is also a maximum surface area, A_{max}, that is allowable before deposition removes reaction products at such a rate that only

partial coating results. The minimum permitted solution concentration is therefore C^*_{hetero}, and the equation [23]

$$r_g = k A_{max} (C^*_{hetero} - C_s) \qquad (4)$$

must also be satisfied.

The maximum yield of coated particles is associated with the maximum ratio of A_{max}/A_{min}, or the equation [23]:

$$A_{max}/A_{min} = 1 + [(C^*_{homo} - C^*_{hetero}) / (C^*_{hetero} - C_s)] \qquad (5)$$

For optimal results and ease of processing, the difference between C^*_{homo} and C^*_{hetero} should be maximized, as well as the difference between C^*_{homo} and C_s. This would ensure that heterogeneous nucleation commenced soon after the solubility limit was surpassed, and also that the homogeneous nucleation limit was far away from the onset of heterogeneous nucleation. These same principles can be applied to the production of coated platelets, whose lower surface area presented processing parameters different from those of whiskers.

3.1.2   Coating of SiC Platelets

Successful coating of SiC platelets was more difficult to obtain than for SiC whiskers. The differences in coating characteristics between the two may be related to the relative surface areas of the two core particles. The average specific surface area of the platelets is an order of magnitude lower than that of the whiskers, which may

have affected the depletion of dissolved Al(III). This effect will now be explained in terms of the coating of SiC platelets with HBAS.

According to the previous explanation of the coating process, coatings are obtained when the pH of the solution is high enough that the given concentration of Al(III) as a hydrolyzed species exceeds its heterogeneous nucleation limit. If sufficient nuclei are produced, the Al(III) drops sufficiently such that the homogeneous nucleation limit is never reached and the present nuclei will grow. Ideally, this is what would occur: HBAS nuclei would cover the entire surface of each SiC particle, at which point nucleation ends and the nuclei grow into thick HBAS coatings. Close to ideal results were obtained with SiC whiskers [6].

The surface area affects the depletion of the Al(III). Note that the homogeneous nucleation limit for a given concentration of Al(III) gets "closer" with time (see figure 1) since the pH will continue to increase as the urea decomposes at a rate determined by the temperature. Therefore, the rate of the increase in pH cannot greatly exceed the relative rate of Al(III) depletion or the homogeneous nucleation limit will be reached.

A reinforcing phase with a high specific surface area provides plenty of sites for heterogeneous nucleation. If added in the proper concentration, this would decrease the Al(III) concentration at a rate in correct proportion to the rate of pH increase, preventing homogeneous nucleation. The result would be thick, uniform HBAS coatings on the SiC without formation of free HBAS particles. A phase with a lower specific surface area would provide fewer sites for heterogeneous nucleation; this nucleation and concurrent

depletion of Al(III) would occur at a slower rate. The pH would then increase at a sufficient rate (offsetting the slower [Al(III)] drop) to reach the homogeneous nucleation limit. This would result in thinner or incomplete coatings on the SiC with many free HBAS particles.

Nearly ideal results were obtained with SiC whiskers with an average aspect ratio of approximately 10; calculations assuming an average whisker diameter of 0.3μm result in a surface area of approximately 2.5cm^2/gm. The platelets used were quite large; they had an average aspect ratio of 8-10 but an average diameter of 25μm, and their surface area was well below 0.5 cm^2/gm (Figure 4). Initial platelet coating runs resulted in uncoated platelets with many free HBAS particles (figure 5(a)). The presence of free HBAS indicated that homogeneous nucleation was occurring in place of heterogeneous nucleation; a situation energetically unfavorable, but possible if the homogeneous nucleation limit is exceeded. This problem was resolved through strict temperature control. A lower processing temperature lowered the rate of urea decomposition, keeping the pH from rising at a critically faster rate than the Al(III) concentration was decreasing. Lowering the temperature approximately 5°C below the whisker coating temperature led to more succcessful coatings (figure 5(b)). Increasing the concentration of platelets so that the total surface area present was close to that of previous whisker runs was not successful due to heavy platelet agglomeration in the solution.

The volume fraction of whiskers or platelets in the final composite was controlled by either varying the concentration of particles added to the coating solution or by using multiple coating

steps, in which a calcined coated powder is added to the solution. In whisker coating runs, summarized in Table 1, both methods were used to produce an array of whisker volume fractions from 10 to 30 vol%. Addition of greater than 5g/l whiskers created large numbers of uncoated whiskers, and addition of less than 2.5g/l whiskers created many free alumina particles [6]. Lower volume fractions were then achieved through a second coating step, using a 5g/l coated powder as the starting particles.

A coating run using platelets yielded a higher volume fraction of platelets or, in other words, a lower total yield of coated powder per concentration of platelets added as compared to whiskers. Application of the maximum whisker core particle concentration of 5g/l to the coating of platelets produced final coated powders with 55 vol% platelets, but they contained large amounts of agglomerated free alumina (Figure 6(a)). Platelets were added in amounts between 5g/l and 20g/l to determine the optimal concentration. As the concentration of platelets was increased to 10g/l, the number of coated platelets remained high while the free alumina particles decreased in number and became less agglomerated (Figure 6(b)). Increases above 10g/l platelets decreased the average size of the free alumina particles, but an increasing number of platelets were only partially coated. Coating runs with more than 20g/l platelets produced significant amounts of uncoated platelets. 10g/l was thus determined to be the optimum platelet concentration.

Coating runs with low platelet additions had a lower limit yield of approximately 55 vol% platelets. Higher platelet additions (up to 20g/l) yielded a coated powder containing more partially coated

platelets, but with much lesser amounts of free alumina. These runs yielded powders as high as 90 vol% platelets. Due to the lower limit, it was necessary to implement additional coating steps in order to decrease the volume fraction of platelets. Coating twice at 10 g/l lowered the final loading of platelets in the coated powder from 60vol% to approximately 45vol% while triple coating yielded approximately 35vol% platelets. Figure 7 shows the double and triple coated powders. Platelet coating data can be seen in Table 1.

In summary, the previous discussion on the effects of surface area on coating can be applied not only to the greater coating difficulty, but also the inability to control yield, as was done with whisker, by varying the core particle concentration in solution. Successful platelet coating runs produced fully coated platelets, but free alumina was still present because the reaction product was not removed quickly enough from solution (Figure 6(b)). Attempts to decrease the platelet concentration only exacerbated this effect. (Figure 6(a)). Increasing the platelet concentration led to partially coated whiskers at the time the homogeneous nucleation limit was reached (Figure 6(d)). Fewer free alumina particles result, however, because the larger surface area present results in less time in the homogeneous nucleation range before the reaction product concentration drops.

3.2 Densification of Coated Powders

3.2.1 Hot Pressing

SiC whisker coated powders were hot pressed to form near fully dense composites. Hot pressed powders contained 10, 17, 21, 25, and 30 volume % whiskers. Greater depth on these results can be found in reference [6].].

SiC platelet coated powders were also hot pressed to near full density. These powders contained between 35 and 65 volume% platelets. Optical micrographs of the dense composites (Figures 8) show the platelets to be well distributed; even at 65 vol% (Figure 8(a)) no agglomerate clusters appear to be present. Figure 9 is a schematic diagram that demonstrates how coated powders may reduce agglomeration. Encapsulation of each reinforcing particle in matrix material precludes the presence of nonsintering inclusion clusters that can be seen in Figure 9(a).

Hot pressing produced a definite platelet orientation. Figure 8 (a), (b), & (d) are taken parallel to the pressing direction. In contrast, Figure 8 (c) is taken perpendicular to the pressing direction. The effect of this orientation on properties will be shown later.

3.2.2 Pressureless Sintering

Pressureless sintering of SiC whisker coated powders resulted in high densities for all whisker loadings. Results for all sintering runs (including those with platelets) are compared with the work of other authors in Table 2. A maximum density of 98% of theoretical was obtained with a 30vol% whisker coated powder. Other densities

ranged between 95 and 97% of theoretical. Sintered densities depended more upon the particular sintering run than the whisker loading. An optical micrograph of the 98% dense sample can be seen in Figure10.

High densities were more difficult to obtain with the SiC platelets. Nevertheless, a maximum density of 95% of theoretical was obtained with a platelet loading of 35 vol% (Figure 10). Attempts to produce densities greater the 90% of theoretical with higher platelet loadings were unsuccessful.

The pressureless sintering results obtained with coated powders are in disagreement with theory on the impossibility of sintering to closed porosity two phase composites with high second phase loading. These theories, most notably that by Lange et al. [4], assumed a mix of discrete matrix particles and reinforcing particles. The schematic diagram in Figure 9 shows how the two mechanisms for matrix constraint during densification can be affected by use of a coated powder. In the mix of discrete particles and whiskers (Figure 9(a)), the matrix must not only sinter to itself but it also must sinter around inclusion clusters, leading to void formation. With coated powders, however, the matrix must only sinter to itself, easing densification.

The high temperatures required for pressureless sintering lead to other problems. Degradation of one of the phases can occur if heated to sintering temperatures in a particular atmosphere or environment. Care must be taken to keep the atmosphere free of oxygen to prevent the conversion of SiC to SiO_2. Degradation of SiC can be a major problem, particularly if sintering in an alumina muffle tube or

metal element furnace. The graphite element furnace used in these experiments, however, presented a serious problem with degradation of the alumina phase. This degradation is caused by a reaction between the alumina and carbon at high temperatures. Figure 11, an Al_2O_3-Al_4C_3 phase diagram, shows that in carbon-containing systems with a small amount of alumina, Al_2O_3+Al_4O_4C will be the stable phases at temperatures above 1700°C. X-ray diffraction of pieces of reacted alumina taken after a sintering run confirmed the presence of Al_4O_4C, along with Al_4C_3, SiC and Al_2O_3 .

Prevention of this reaction, necessary for successful pressureless sintering, is made more difficult by the high vapor pressure of carbon. The green compact must be protected from the carbon in the furnace environment. This was achieved through two steps. First, the compacts were placed in a large, closed SiC crucible or an Al_2O_3 crucible "painted" with an SiC-water slurry. Inside the crucible, the compacts were then packed in a 50/50 mix of Al_2O_3 and SiC powders. Sintering results showed reaction of the alumina on the outside of the powder bed, but degradation of the sintered compact was greatly reduced or eliminated.

For optimal sintering results, it is necessary that the green compact be as dense as possible prior to firing. When uniaxially pressed, compact cracking and end capping can result. During sintering, this combines with the damage created by inclusions [22] to create a defective sintered part. Damage was minimized here by application of just enough uniaxial load for structural integrity followed by a large isostatic pressure. Green compact densities were approxiately 50% of theoretical without noticeable damage. Further

improvements in sintering results could be obtained by wet processing or other methods to produce high density green bodies with a minimum of flaws that could lead to serious damage in the sintered piece.

3.3 Mechanical Property Testing

3.3.1 Coated Whisker Composites

The fracture toughness values for the coated whisker composites ranged between 4 and 6 MPa√m in the hot pressed composites and 5 and 7 MPa√m in the free sintered composites. As expected, the fracture toughness values were lower for composites with light whisker loading and increased with whisker volume percent. Fracture toughness data are shown in Figure 12.

The pressureless sintered composites showed slightly greater toughnesses than the hot pressed composites. One factor that may have contributed to this is the greater porosity of the pressureless sintered composites; Tiegs and Becher [3], in a study of pressureless sintered Al_2O_3-SiC whisker composites, showed the maximum toughness for 10vol% whisker composites to occur at a density of 92% of theoretical. They measured decreasing toughnesses up to the maximum 99% density, and suggested that crack propagation was inhibited by residual porosity as well as the whiskers. If this mechanism is correct, it would certainly apply here; tested pressureless sintered composites were an average of 95% dense, whereas hot pressed composites were 98% dense on average.

Other work, however, shows the effect of porosity on hot pressed Al_2O_3-SiC composites to be just the opposite. One study with 30vol% whisker composites demonstrated fracture toughness to increase as a function of increasing theoretical density [24]. Another study of fracture resistance (R curve) behavior with 25wt.% SiC whiskers indicated a rise in fracture resistance with a decrease in porosity, using porosities ranging from 0.6% to 11.5% [25]. It appears that the greater porosity of the pressureless sintered composites cannot be reliably invoked to explain their greater toughness.

In Figures 14(b) and 15(b), the pressureless sintered samples, appear to have larger, more intact grains than the hot pressed samples. The difference in grain size may have affected the fracture toughness measurements, but does not explain the different appearance of the fracture surfaces. The more intact appearance of the grains in the pressureless sintered samples suggest that crack propagation occurred in an intergranular rather than a transgranular mode. This intergranular fracture could be the result of the remains of an Al-Y-Mg-Si-O glassy phase formed by the liquid phase-inducing sintering aids pooling at the grain boundaries. The glassy phase at these boundaries would prove a preferable pathway to an advancing crack, with the hindrance to propagation resulting from the more sinuous crack path required.

The difference in grain size is the result of the higher processing temperatures required for pressureless sintering causing greater grain growth. The larger grains of the pressureless sintered sample should, however, result in lower fracture strength (and hence lower

fracture toughness) from the Orowan relation

$$\sigma_f = k / \sqrt{d} \qquad (6)$$

where fracture strength increases with decreasing grain size d. As the grain size discrepancy produces results contrary to theory, this cannot explain the greater toughness of the pressureless sintered composites.

Differences in whisker length and orientation existed between the pressureless sintered and the hot pressed composites. In the hot pressed composites, the whisker orientation was quite uniform in the plane of the pressing direction (whisker length perpendicular to the pressing direction) as shown in Figure 13. The pressureless sintered composites showed less uniform orientation, as they were dry pressed at low pressures before isostatic pressing and pressureless sintering (Figure 10 (a)). In addition to less uniform orientation, the microstructure in Figure 10(a) also shows the possibility of more broken whiskers than the hot pressed composites, a result of the high isostatic pressures required for green body densification. Shorter whiskers and less uniform orientation would seem to produce lower toughness values, so here again the results contradict the microstructural clues.

The best properties of the hot pressed and pressureless sintered composites were inferior to those of the toughest Al_2O_3-SiC whisker composites. Wei and Becher obtained toughnesses as high as 9.0 MPa$\sqrt{m}$ with hot pressed 20 vol% whisker composites [1]. However, it should be noted that they measured a fracture toughness of 4.6 MPa$\sqrt{m}$ for the monolithic alumina used in the study. Hot pressed

samples of homogeneously precipitated alumina produced fracture toughnesses of around 3.1 MPa√m. The quality of the powder produced as a coating is apparently not equal to that of the finest grades of alumina powder, producing inferior composite properties. The whiskers used on this study were also of suspect quality, with jagged surfaces. This may have caused mechanical "keying" into the matrix, preventing whisker pullout. Many whiskers showed little tendency to debond in the face of an advancing crack, preferring instead to fracture; a trait most noticeable from the cracks produced by Vicker's indents.

3.3.2 Coated Platelet Composites

Fracture toughness values of the hot pressed platelet composites ranged between 4 and 7.5MPa√m for all volume percent platelets whether they were hot pressed or pressureless sintered. Values for hot pressed composites with the load applied perpendicular to the hot pressing direction were slightly lower in this range. Larger platelet loadings did not produce noticeable increases in average toughness, even though a few samples reached values close to 8MPa√m. Average toughnesses for the platelet composites can be seen in Figure 16. Bend strengths ranged between 300 and 600MN for all platelet loadings tested. Again, volume percent and densification method did not have a large effect on the values obtained. Samples tested with the load applied perpendicular to the pressing direction had slightly lower strengths. Average bend strengths are plotted in Figure 18.

Apparently, the only microstructural trait with a noticeable effect on the mechanical properties was the orientation of the platelets. Application of the load perpendicluar to the original hot pressing direction resulted in a decrease of about 25% in the measured properties. Figures 17 shows the composite fracture surfaces. When load was applied perpendicular to the hot pressing direction the crack was able to propagate along the surface of the platelets (Figure 17(b)). Loading the sample parallel to the pressing direction resulted in cracks propagating across the long axis of the platelets (Figure 17(a)). Obviously, skimming along the surface of a platelet is much easier than going through or around one, and the measured properties reflected this accordingly.

Note that the fracture surfaces are very rough and there are very few, if any, broken platelets. This suggests that crack propagation occurred almost entirely at the Al_2O_3-SiC interface. The strength of the surface-coating interface will eventually have to be investigated as in the future this may turn out to be the property limiting factor.

The large deviations in fracture toughness and bend strength values and the lack of dependence of these values upon the microstructure indicates an overriding factor controlling the properties, most likely the internal flaws produced in processing. This problem is magnified with the use of these platelets because of their large size (average 25μm diameter). Larger inclusions will produce larger internal flaws, stemming from the excluded volume during green compact formation and the alumina - silicon carbide thermal expansion mismatch creating microcracks in the composite upon cooling. Note that in the optical micrographs of the densified

samples the flaws that are present are quite large, reaching 25μm in diameter (which is, incidentally, the average size of the platelets used). These problems could be lessened by use of smaller platelets or by improvements in the green state resulting in less defects in the fired piece.

The fracture toughness and bend strength values were lower than expected for heavily loaded Al_2O_3-SiC composite materials, even for the best samples. This could again be due to the powder produced during precipitation possessing inferior mechanical properties to the better Al_2O_3 powders available. Improvements in properties could then be obtained by using sedimentation to rid the coated powder of free alumina particles, leaving only the coated platelets. Better Al_2O_3 powder grades could then be mixed with the coated platelets, placing them in a superior matrix. Improvement of these platelet composite properties will be the topic of future work.

4. Conclusion

Coated powders have proved to be a viable method for the fabrication of microcomposites, and present several advantages over the convential discrete particle/particle processing. These advantages are:

(1) Reduction of barriers to densification. Hot pressing was achieved under relatively mild conditions compared to those of other authors. Pressureless sintering to closed porosity, thought to be

impossible with reinforcing volume fractions greater than 20%, was successful with up to 30 vol% whiskers and 35 vol% platelets.

(2) A more homogeneously distributed matrix. The coating reduces reinforcing particle contacts, thus eliminating homogeneity-destroying agglomerates.

(3) The coated powder is immune to the problem of phase separation after mixing, unlike discrete particle composite amalgamations.

All of these benefits apply for the coated whisker powders, but because of the coating characteristics of the platelets (the lack of surface area producing a significant amount of free alumina) the problem of settling is still present, albeit in a reduced fashion. Because of the move away from whiskers due to health and safety reasons, platelets have increased relevance as a reinforcing phase. Better understanding of the coating process is needed to produce thicker coatings on the platelets and reduce the presence of free alumina in the final powder if so desired.

Mechanical properties, while not as good as those produced by other authors, are encouraging since a significant increase in toughness over the monolithic homogeneously precipitated Al_2O_3 was attained. Two areas where modifications could result in increases in fracture toughness are the indigenous defects in the composite after densification and the quality of the matrix alumina. With the latter, a coated platelet powder with most of the free alumina sedimented out (platelet loading of about 90 vol%) could be mixed with varying amounts of high grade alumina powder to create mixes with a range of platelet loadings and possibly superior properties. Ridding the

compact of its indigenous defects would be more difficult; smaller inclusions or improvements in the green state via methods such as wet processing could lead to better overall properties.

References

(1)   G.C. Wei and P.F. Becher, "Development of SiC Whisker-Reinforced Ceramics," *Am. Ceram. Soc. Bull.* Vol.64, No.2 (1985) p.298-304.

(2)   J.H. Porter, F.F. Lange and A.H. Chokshi, "Processing and Creep Performance of SiC-Whisker-Reinforced Al_2O_3," *Am. Ceram. Soc. Bull.* Vol.66, No.2 (1987) p.343-347.

(3)   T.N. Tiegs and P.F. Becher, "Sintered Al_2O_3-SiC Whisker Composites," *Am. Ceram. Soc. Bull.* Vol.66, No.2 (1987) p.339-342.

(4)   F.F. Lange, L. Atteraas and F. Zok, "Deformation Consolidation of Metal Powders Containing Steel Inclusions."

(5)   D. Kapolnek and L.C. DeJonghe, "Particulate Composites from Coated Powders," to be published.

(6)   D. Kapolnek, "Synthesis of Alumina-Coated Whiskers for Production of SiC Whisker Reinforced Alumina Composite Materials," M.S. Thesis, UC Berkeley Dept. of Mat. Sci. and Eng. and Center for Advanced Materials, Materials and Chemical Sciences Division, LBL.

(7)   M. Akinc and D. Sordelet, "Preparation of Yttrium, Lanthanum, cerium, and Neodymium Basic Carbonate Particles by Homogeneous Precipitation," *Adv. Cer. Matls.* Vol.2, No.3A (1987) p.232-238.

(8) M. Akinc, D. Sordelet, and M. Munson, "Formation, Structure, and Decomposition of Lanthanide Basic Carbonates," *Adv. Cer. Matls.* Vol.3, No.3 (1988) p.211-216.

(9) E.A. Barringer and H.K. Bowen, "High-Purity, Monodisperse TiO_2 Powders by Hydrolysis of Titanium Tetraethoxide. 1.Synthesis and Physical Properties," *Langmuir* Vol.1, No.4 (1985) p.414-420.

(10) M. Ankinc and A. Celikkaya, "Preparation of Yttria Powders by Emulsion Precipitation," in *Advances in Ceramics,* Vol.21: Ceramic Powder Science, (1987) p.57-67.

(11) J.H. Jean and T.A. Ring, "Processing Monosized TiO_2 Powders Generated with HPC Dispersant," *Am. Cer. Soc. Bull.* Vol.65, No.12 (1986)   p.1574-77.

(12)   J.H. Jean and T.A. Ring, "Nucleation and Growth of Monosized TiO_2 Powders from Alcohol Solution," *Langmuir* Vol.2, No.2 (1986) p.251-55.

(13)   M. Mitomo and Y. Yoshioka, "Preparation of Si_3N_4 and AlN Powders from Alkoxide-Derived Oxides by Carbothermal Reduction and Nitridation," *Adv. Cer. Matls.* Vol.2, No.3A (1987) p.253-256.

(14)   K. Uchiyama, T. Ogihara, T. Ikemoto, I Mizutani, and M. Kato, "Preparation of Monodispersed Y-Doped ZrO_2 Powders," *J. Matls. Sci.* Vol.22 (1987) p.4343-4347.

(15)   J.E. Blendell, H.K. Bowen, and R.L. Coble, "High Purity Alumina by Controlled Precipitation from Aluminum Sulfate Solutions," *Am. Cer. Soc. Bull.* Vol.63, No.6 (1984) p.797-801.

(16)   B.C. Cornilsen and J.S. Reed, "Homogeneous Precipitation of Basic Aluminum Salts as Precursors for Alumina," *Am. Cer. Soc. Bull.* Vol.58, No.12 (1979) p.1199.

(17)   C.F. Baes and R.E. Mesmer, The Hydrolysis of Cations, p.112-122, John Wiley and Sons, Inc. New York, N.Y., 1976.

(18)   H.N. Willard and N.K. Tang, "A Study of the Precipitation of Aluminum Basic Sulfate by Urea," *J. Am. Chem. Soc.* Vol.59 (1937) p.1190-1196.

(19)   L. Gordon, M.L. Salutsky, and H.N. Willard, Precipitation from Homogeneous Solution, Chapter 2, "Precipitation of Hydroxides and Basic Salts," John Wiley and Sons, Inc., New York, N.Y., 1959.

(20)   P.C. Paris and G.C. Sih, "Stress Analysis of Cracks," from Fracture Toughness Testing and its Applications, ASTM STP381, 1965, p.30-81.

(21)   P.C.Paris and G.C. Sih, "Stress Analysis of Cracks," from Fracture Toughness Testing and its Applications, ASTM STP 381, 1965, p.30-81.

(22)   L.C. DeJonghe and M.N. Rahaman, "Densification   of Particulate Composites: The Role of Heterogeneities," *Mat. Res. Soc. Symp. Proc.*, Vol.155 (1989) p.353-361

(23) A.K. Garg and L.C. De Jonghe, "Microencapsulation of Silicon Nitride Particles with Yttria and Yttria-Alumina Precursors," *J. Mater. Res.* Vol.5, No.2 (1990) p.136-142.

(24) J. Homeny, W.L. Vaughn, and M.K. Ferber, "Processing and Mechanical Properties of SiC-Whisker-Al_2O_3-Matrix Composites, *J. Am. Cer. Soc. Bull.* Vol.66, No.2 (1987) p.333-338.

(25) R.F. Krause, Jr. and E.R. Fuller, Jr., "Fracture Resistance Behavior of Silicon Carbide Whisker-Reinforced Alumina Composites with Different Porosities," *J. Am. Cer. Soc.* Vol.73, No.3 (1990) p.559-66.

(26) M.D. Sacks, H.W. Lee, and O.E. Rojas, "Suspension Processing of Al_2O_3/SiC Whisker Composites," *J. Am. Ceram. Soc.* Vol.71, No.5 (1988) p.370-379.

(27) L.M. Foster, G. Long, and M.S. Hunter, *J. Am. Ceram. Soc.*, Vol.39, No.8 (1956)

Appendix

Equipment List

Chemicals: Aluminum Sulfate: Fisher Scientific, Inc.
Fair Lawn, NJ

Urea: J.T. Baker Chemical Co.
Phillipsburg, NJ

SiC Whiskers: American Matrix, Inc.
Knoxville, TN

SiC Platelets: C-Axis Technology, Inc.
Jonquiere, Quebec, Canada

Dispersant: PVP K30 GAF Chemical Co.
Wayne, NJ

X-Ray Diffractometer: Siemens Krystalloflex

SEM: International Scientific Instruments, Inc., Santa Clara, CA
(DS-130 SEM)

Hot Press and Sintering Furnace: Thermal Technologies, Inc.,
Concord, NH

Optical Microscope: Nikon Epiphot-TME
Nippon Kokagu K.K.

Table 1: Initial core particle concentration in solution versus final particle loading in the densified composites

Core Particle	Concentration in Solution (gm/l)	Final Loading in Dense Composite (Volume %)
Whiskers	5.0	30
Whiskers	4.3	25
Whiskers	3.6	21
Whiskers	2.9	17
Coated Whiskers	5.0	10
Platelets	2.5	55
Platelets	5.0	55
Platelets	10.0	60
Platelets	15.0	80
Platelets	20.0	90
Coated Platelets	10.0	45
Twice Coated Platelets	10.0	35

Table 2: Pressureless sintering results for various volume fractions of whiskers and platelets. Results of other authors are included for comparison.

Reinforcement	Volume %	Final Density (% of theoretical)
Whiskers	30	98
Whiskers (Sacks et.al.[26])	30	80
Whiskers	25	95
Whiskers	21	96
Whiskers (Tiegs & Becher[3])	20	85
Whiskers	17	97
Whiskers (Sacks et.al.[26])	15	83
Whiskers	10	96
Whiskers (Tiegs & Becher[3])	10	95
Platelets	35	95

line 1: solubility limit

line 2: heterogeneous
         nucleation limit

line 3: homogeneous
         nucleation limit

3
2
1

Concentration in Solution

pH

- - - - - - - -   heterogeneous nucleation and growth only
. . . .   homogeneous and heterogeneous
                          nucleation and growth
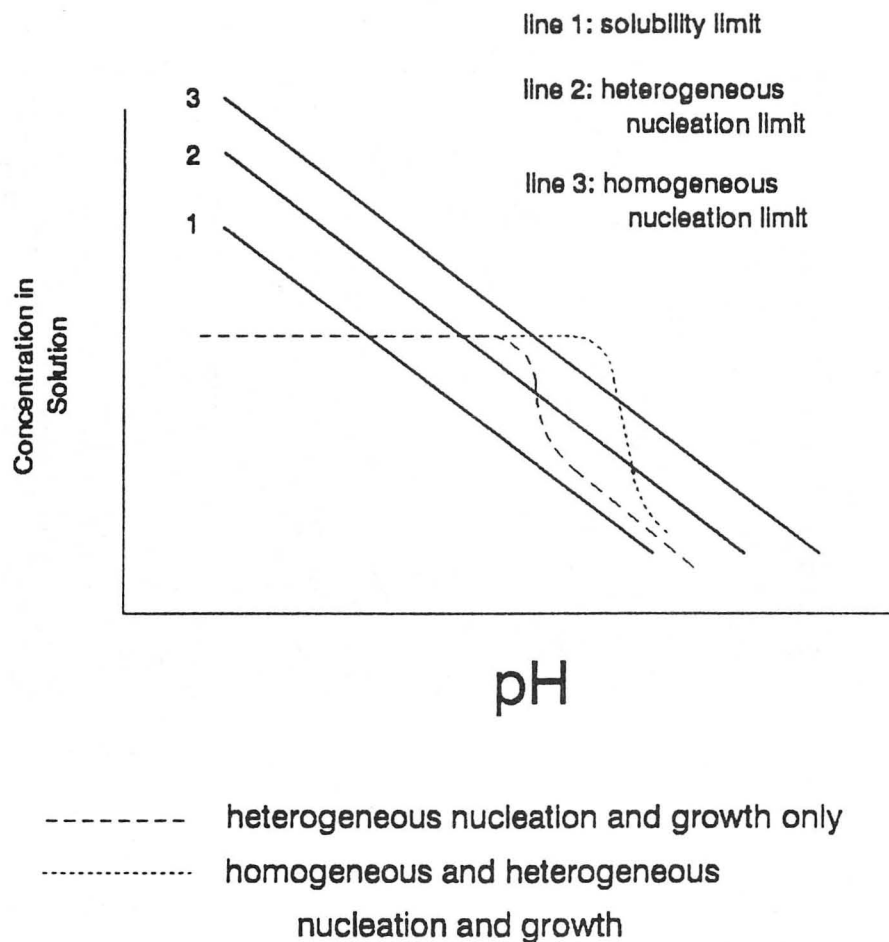
XBL 9012-4002

Figure 1: Modified LaMer Diagram showing the nucleation and growth behavior of a precipitate from solution with increasing solution pH (from Blendell et. al. [18]).
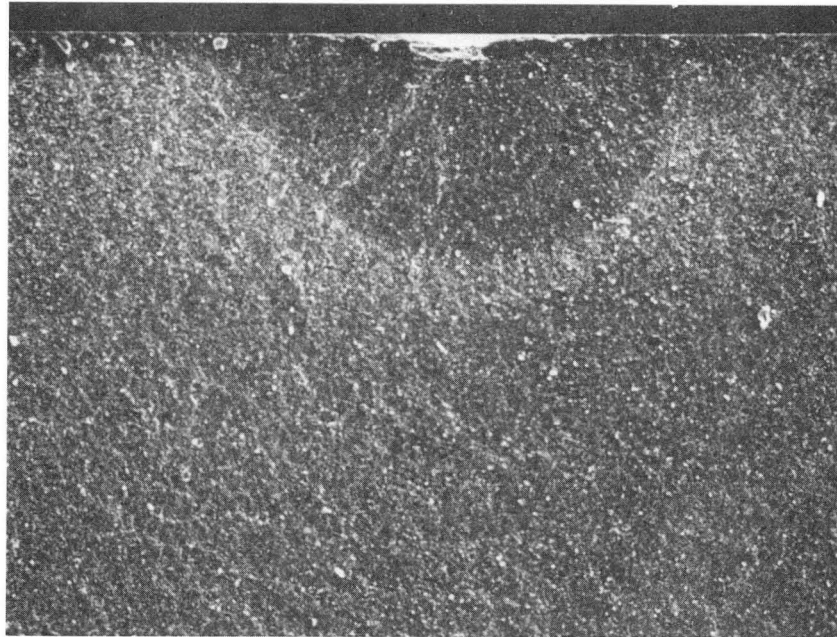
100μm

XBB900–10171

Figure 2:   A Knoop indent-induced elliptical flaw for fracture
toughness   measurements.

Concentration vs Time

- C_{lim} — Critical Limiting Supersaturation
- C_{homo}^{*} — Rapid Homogeneous Nucleation
- C_{hetero}^{*} — Growth by Diffusion
- C_{s} — Solubility

Regions: I, II, III; curves a, b, c
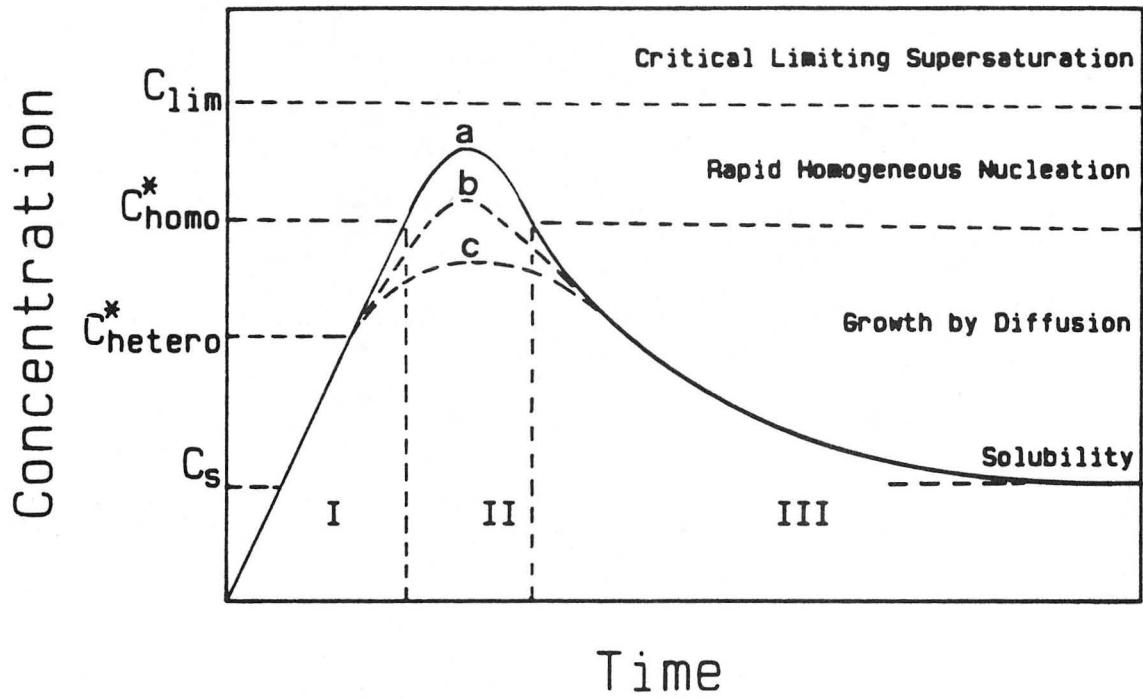
XBL 9012-4003

Figure 3: Modified LaMer diagram of the nucleation and growth behavior of a precipitate from solution for the microencapsulation of fine particles.
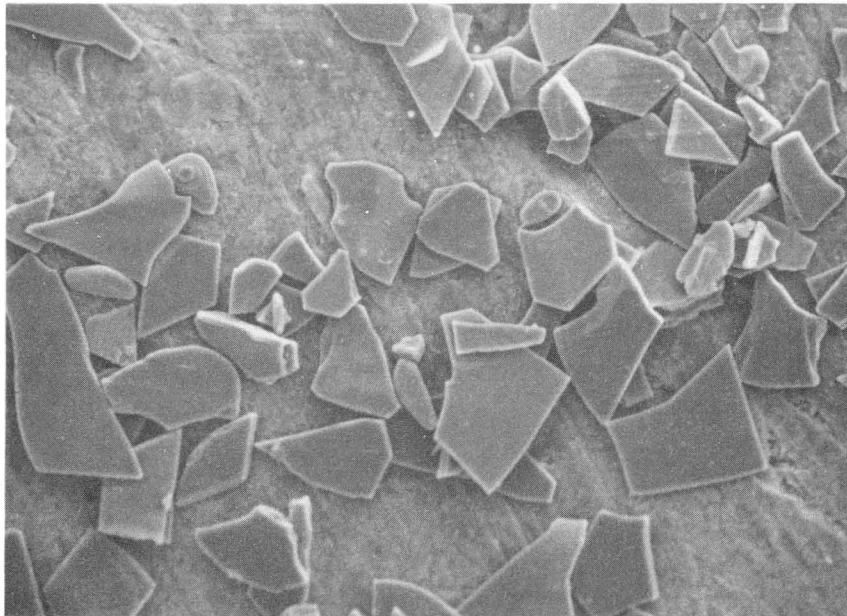
25µm

Figure 4: SiC platelets used in these experiments. Average size is 25um.

5a

25μm

5b
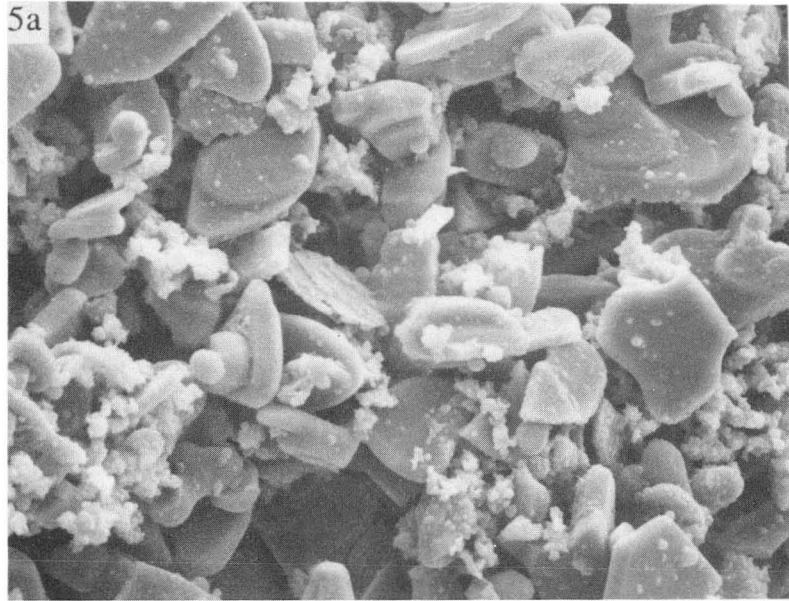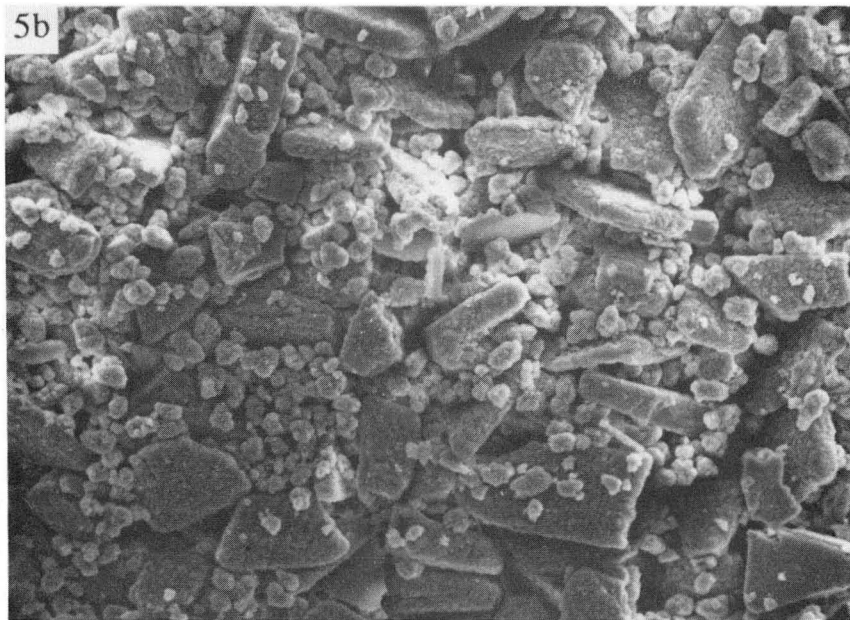
XBB900-10173

Figure 5: Results of initial coating runs using 2.5 g/l platelets. (a) Unacceptable results with many uncoated platelets (b) Acceptable coating results.

6a

20μm

6b
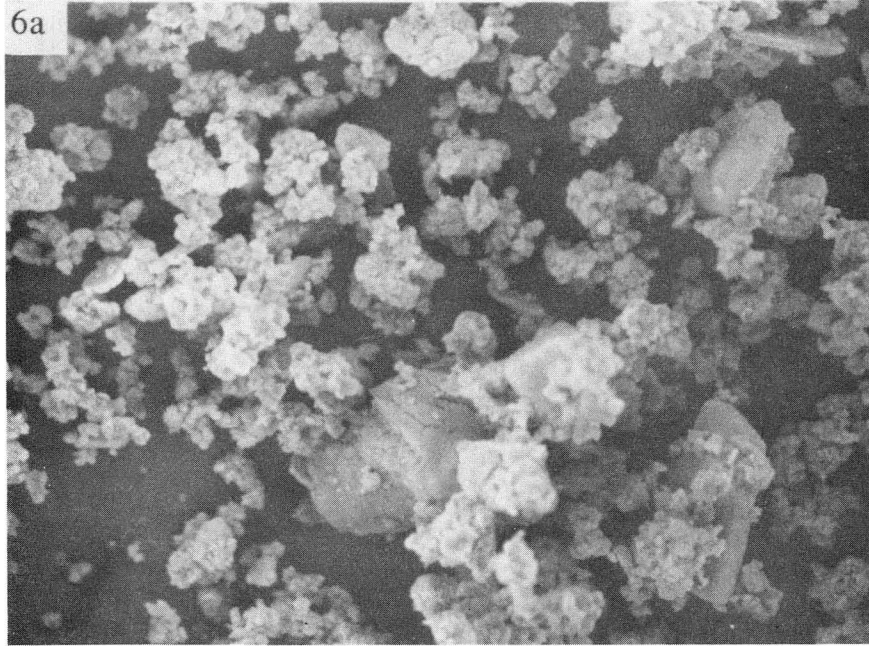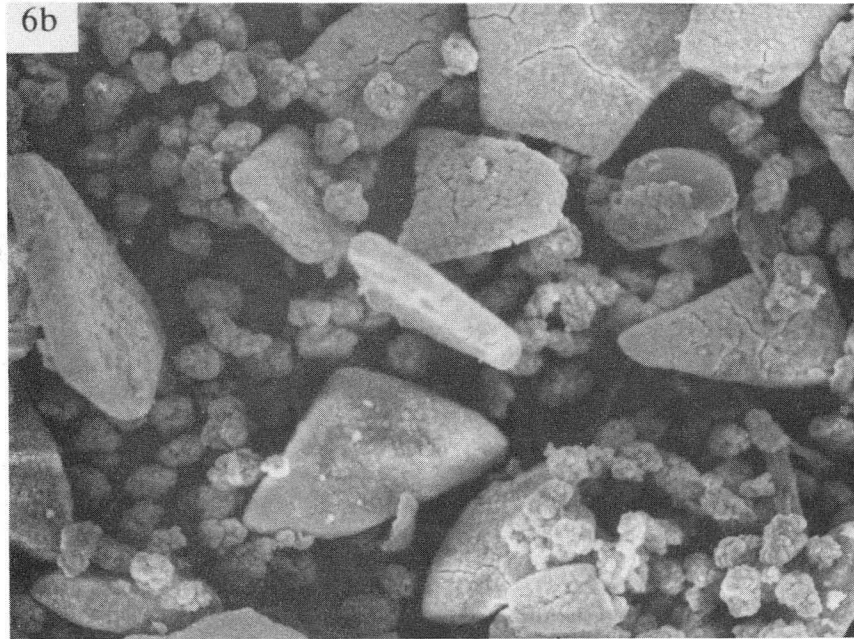
XBB900–10174

Figure 6: Coating results with varying platelet concentrations. (a) 5g/l (b) 10g/l (c) Thickness of optimal 10g/l platelet coating (d) 20g/l.

6c

$2\mu m$

6d

$20\mu m$

XBB900−10175

39
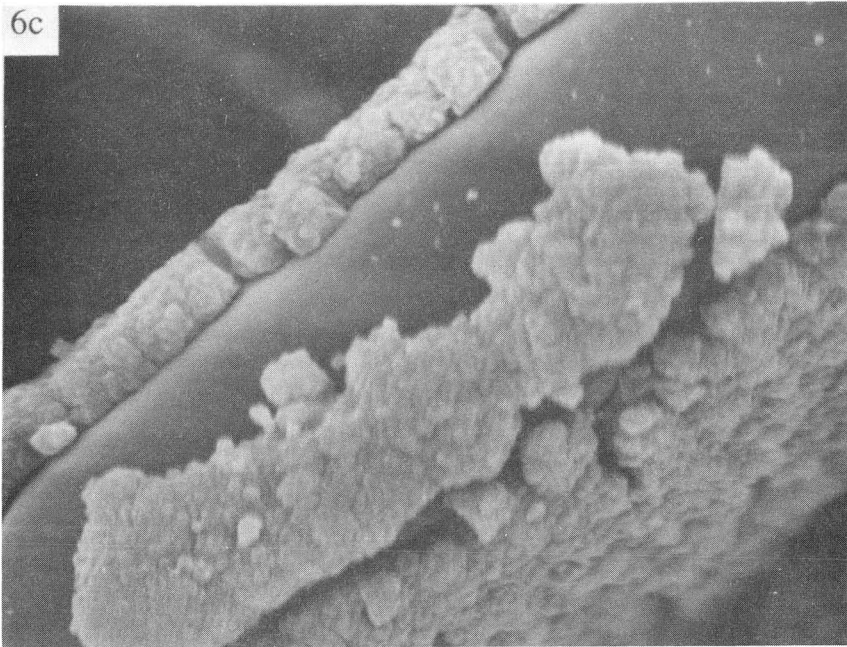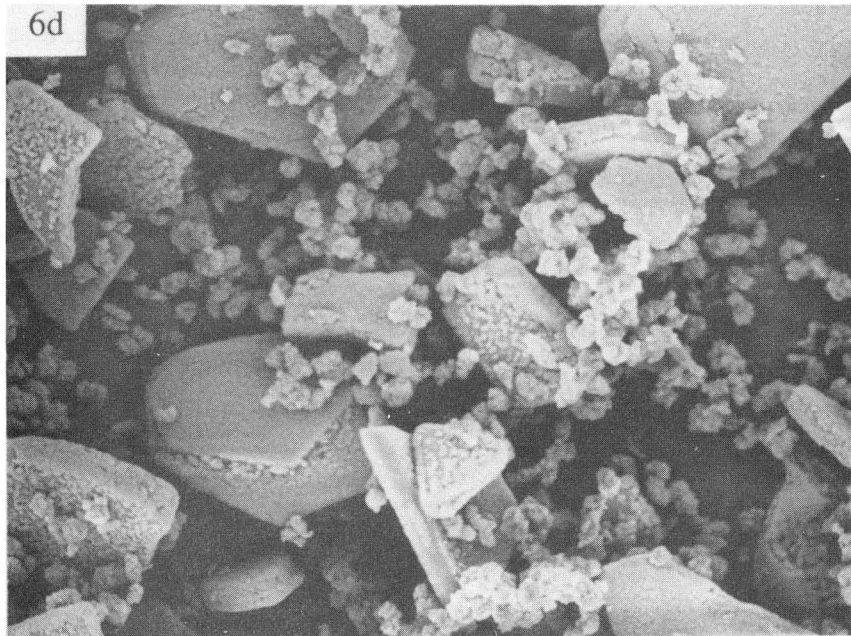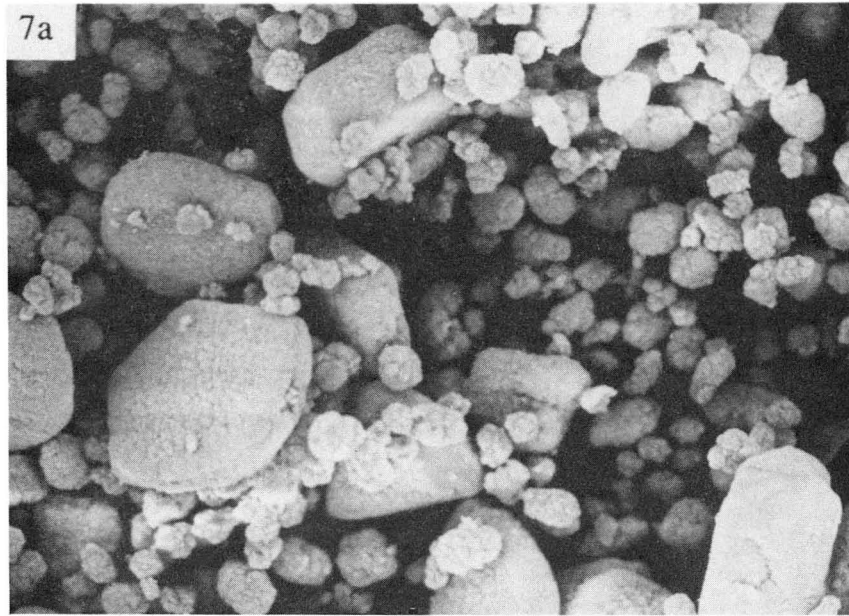
20μm
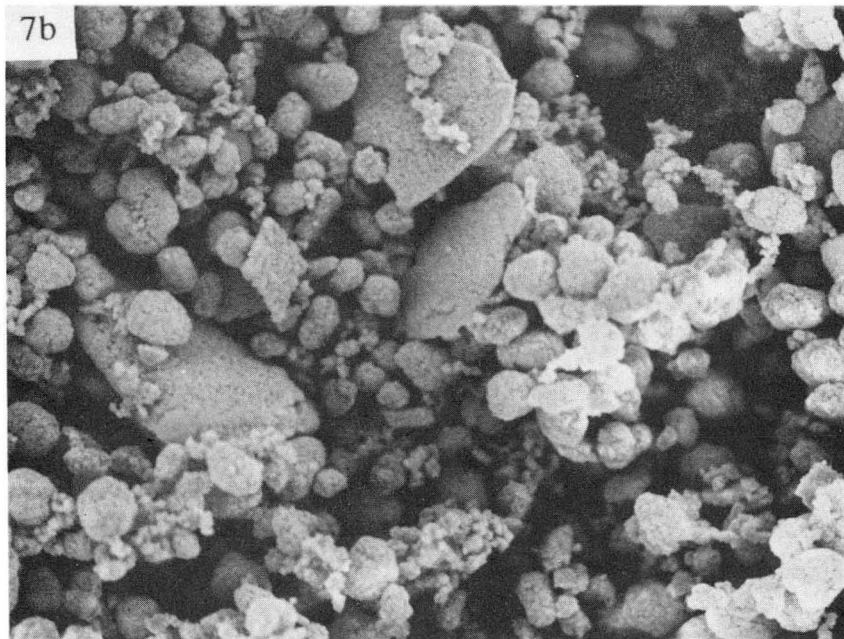
XBB900-10176

Figure 7: Coating results with multiple coating steps. (a) 10g/l, coated twice (b) 10g/l, coated three times.

8a

25μm

8b
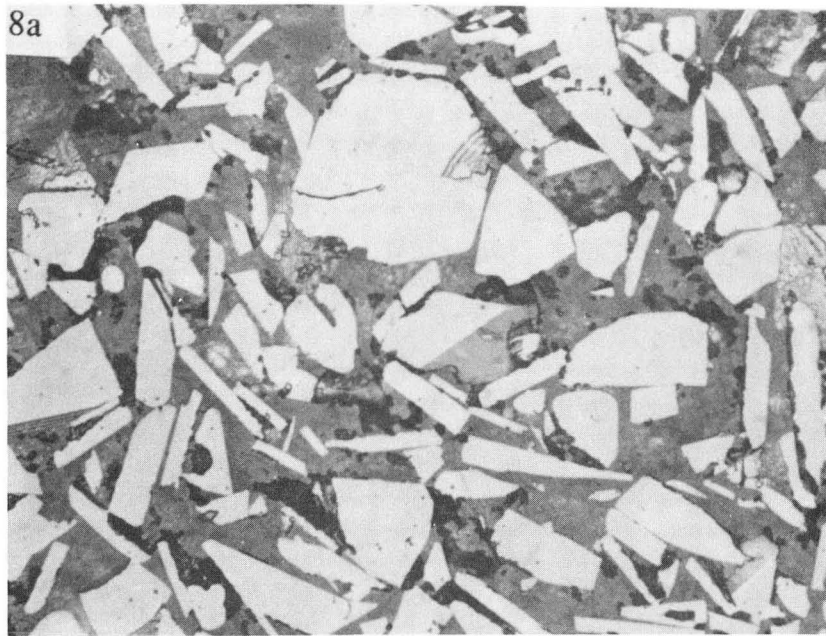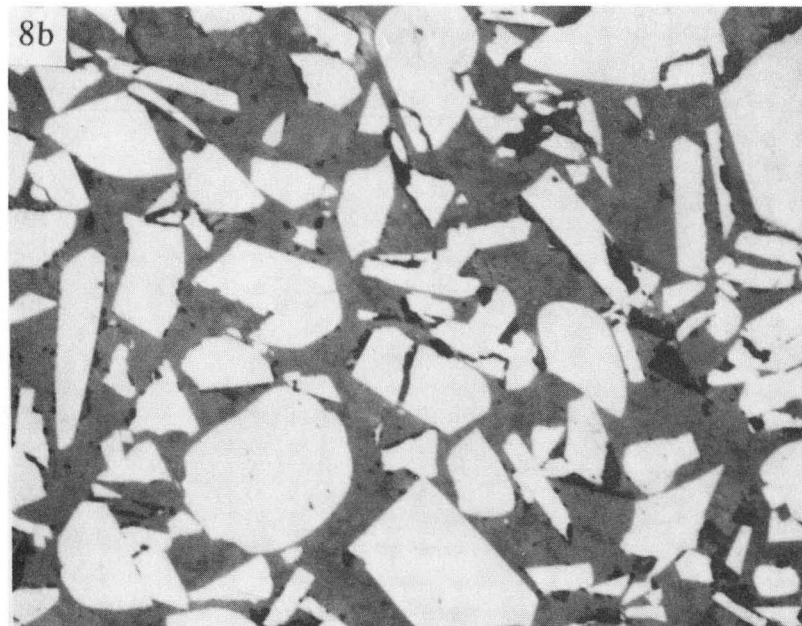
XBB900-10177

Figure 8: Hot pressed coated platelet composites. (a) 60vol%
platelets (b) 45vol% platelets (c) 45vol% platelets, taken
perpendicular to the hot pressed direction (d) 35vol% platelets.

41

8c

25μm

8d

XBB900–10178

SiC whisker

Alumina matrix

Voids
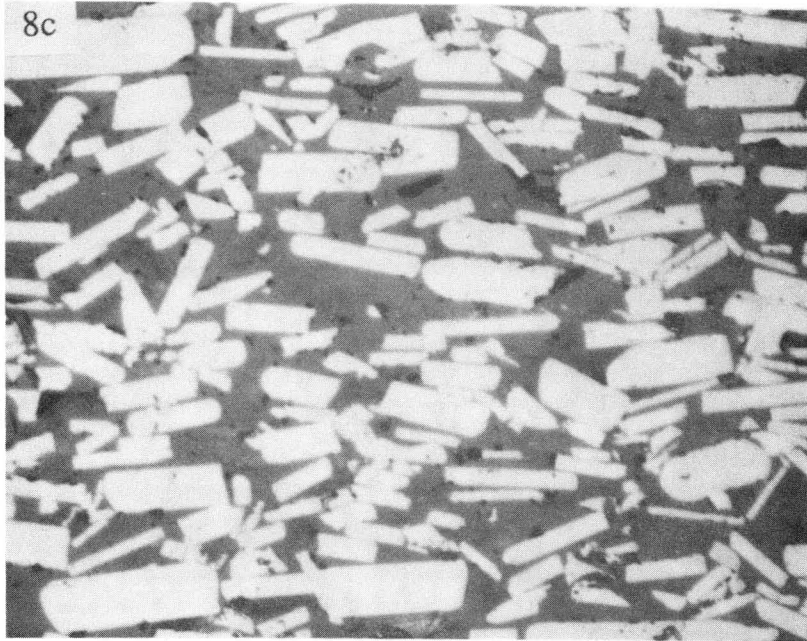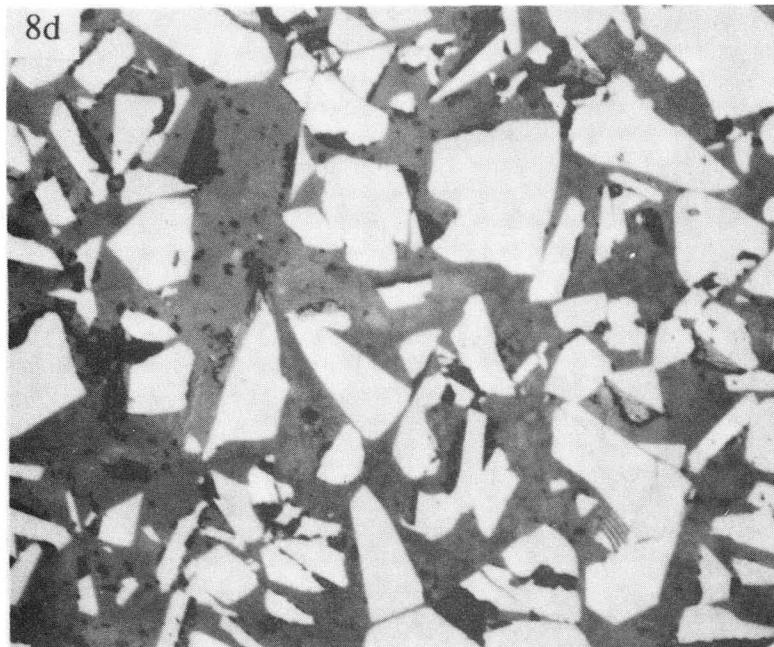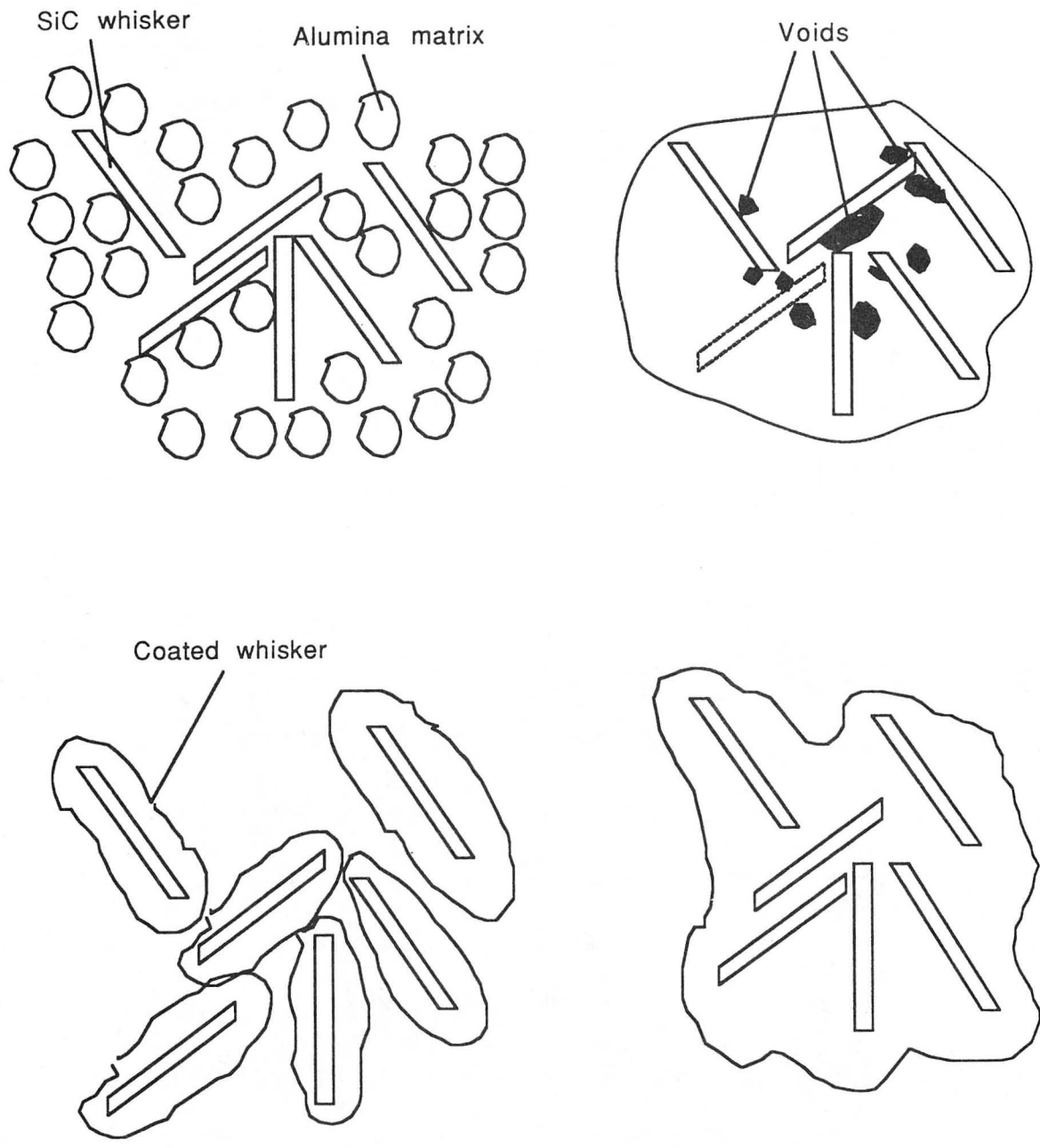
Coated whisker

XBL 9012-4004

Figure 9: Schematic of the effect of coated particles on densification for two phase microcomposites. (a) discrete particle/whisker mix before and after densification (b) coated whiskers before and after densification

43
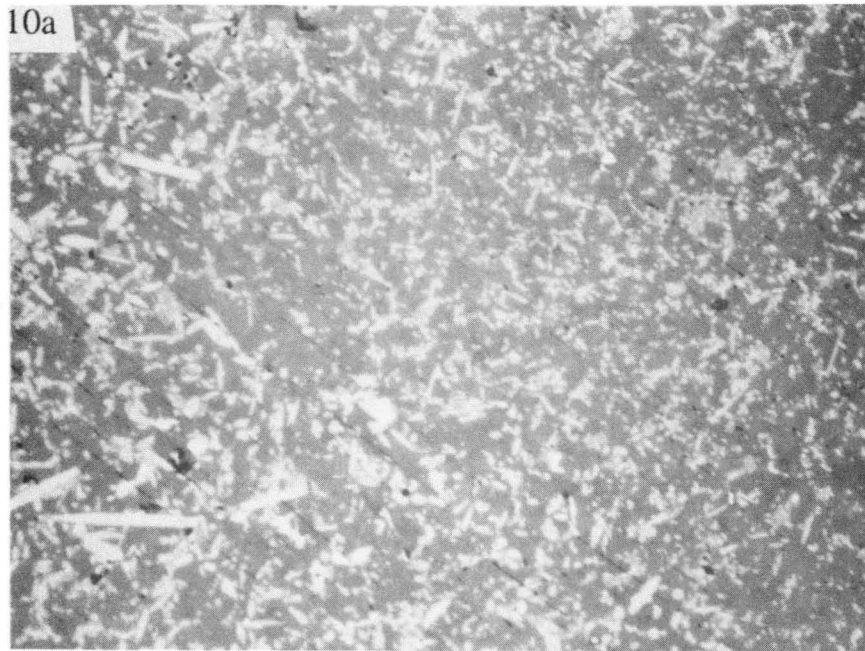
25μm
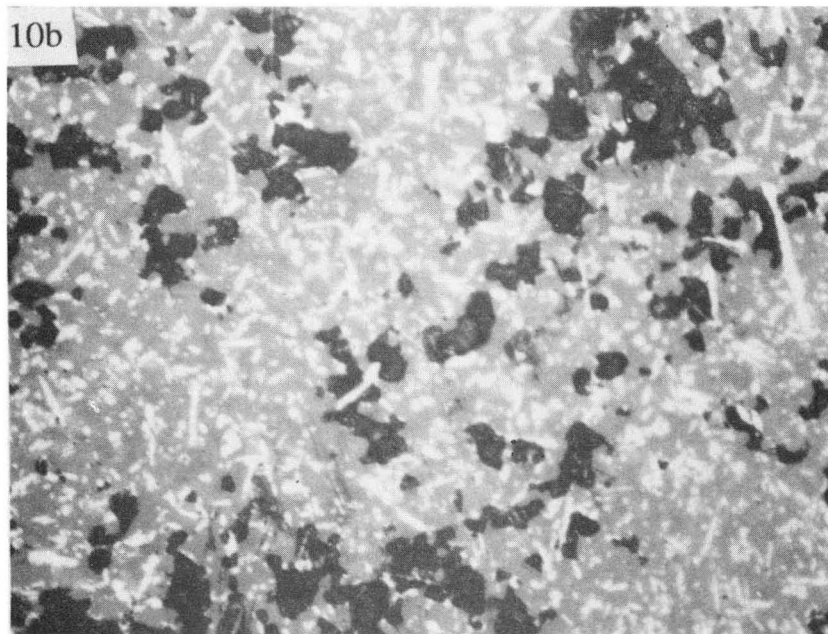
XBB900-10179

Figure 10: Pressureless sintered coated powder composites.compared with discrete particle mix composites (a) coated powder, 30vol% whiskers (b) discrete mix, 30vol% whiskers (c) coated powder, 35vol% platelets (d) discrete mix, 35vol% platelets

44

10c

25μm

10d
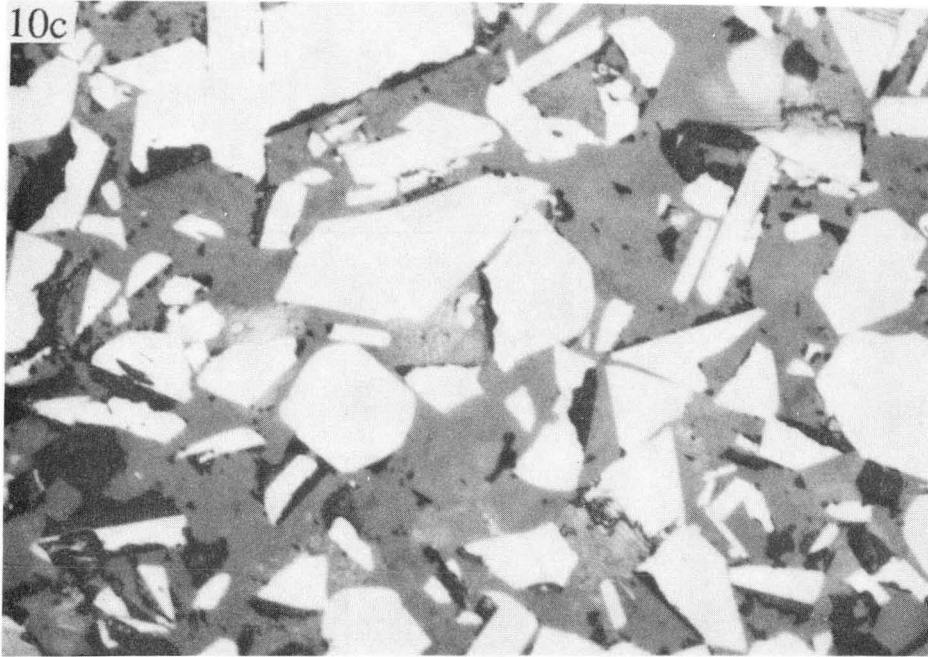
XBB900-10180

Al$_2$O$_3$–Al$_4$C$_3$
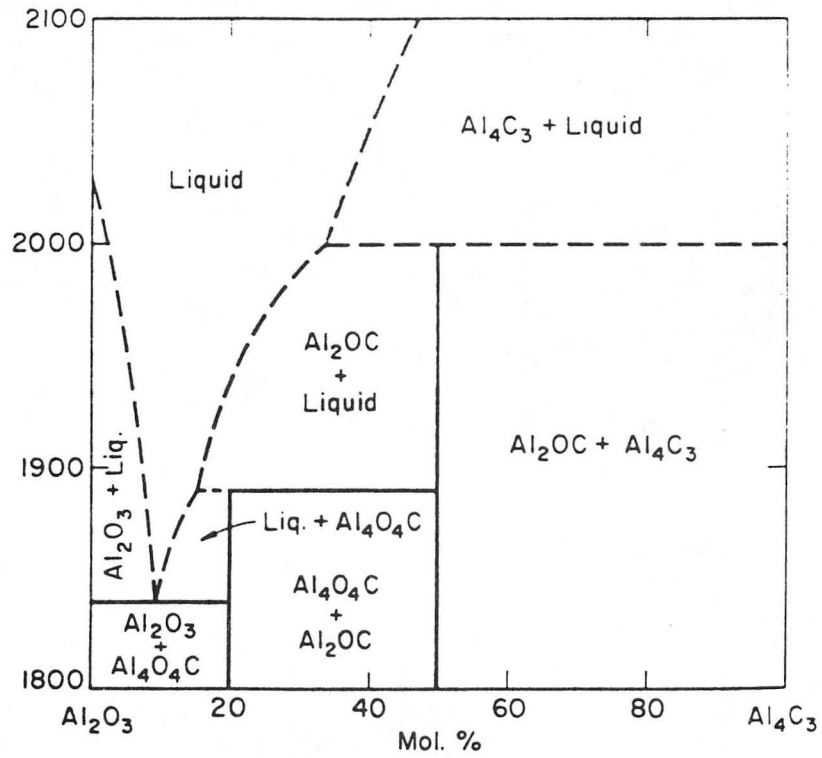
Figure 11: Phase diagram for the Al$_2$O$_3$-Al$_4$C$_3$ system (from Foster et.al. [27].
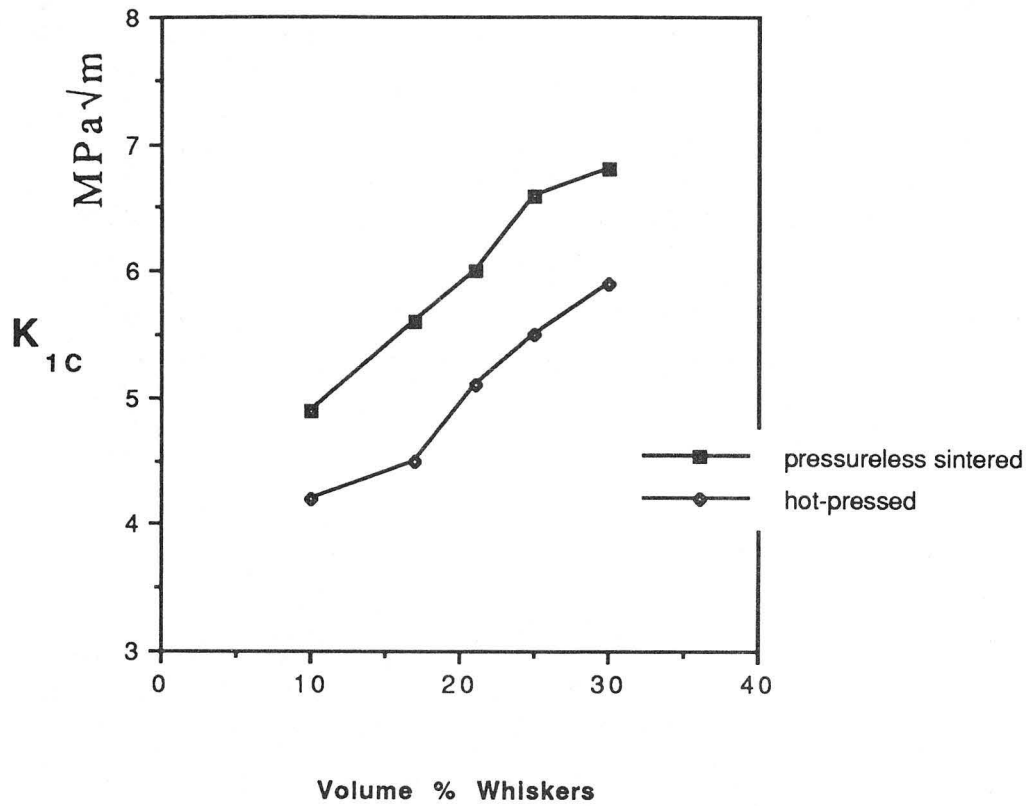
46

Figure 12: Average fracture toughnesses of hot pressed and pressureless sintered coated whisker composites.
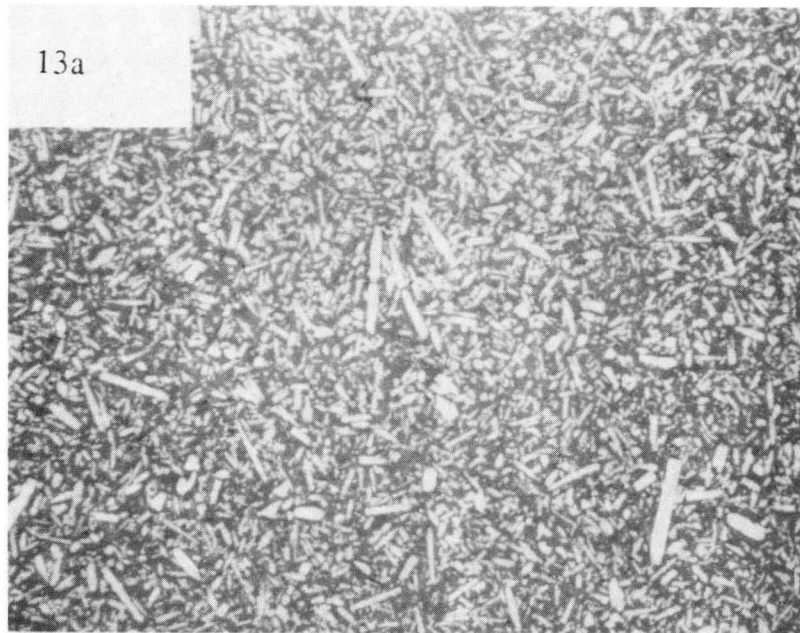
20μm
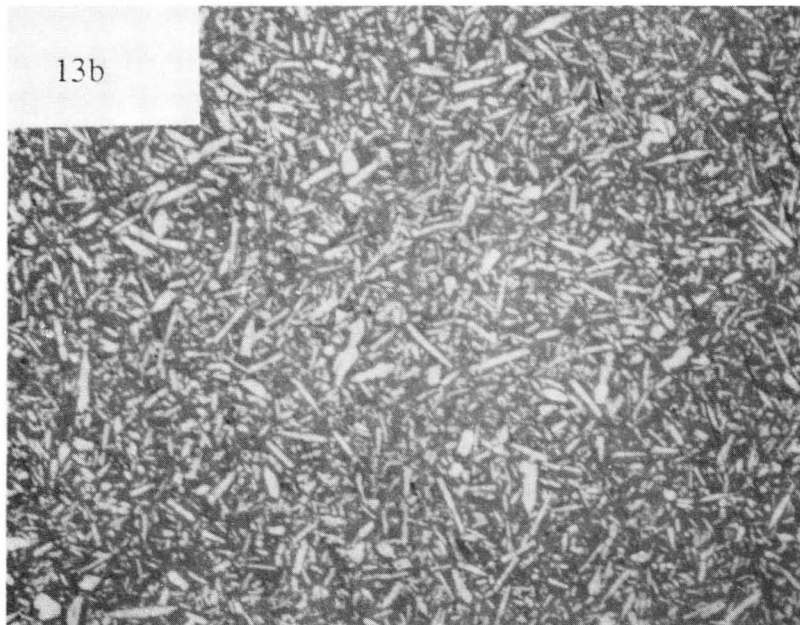
XBB890-9501B

Figure 13: Hot pressed coated whisker composites. (a) 30vol% (b) 25vol%.
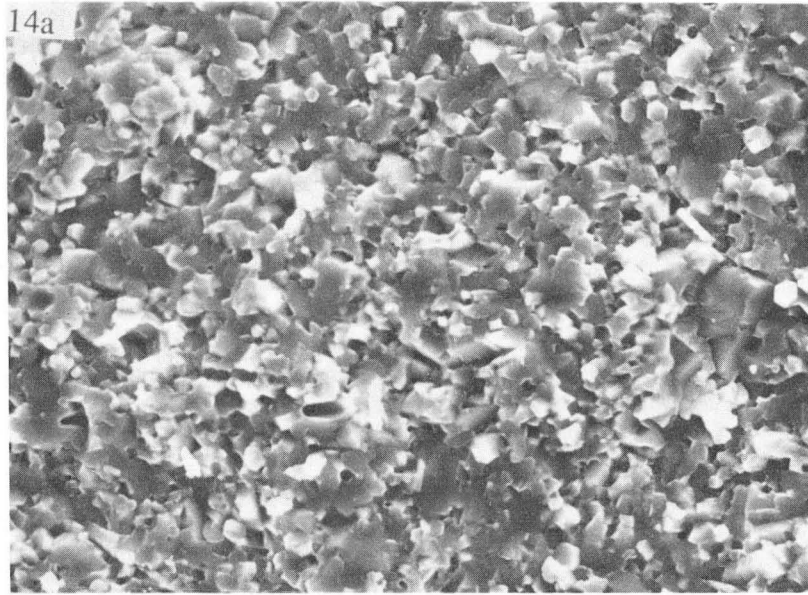
5μm
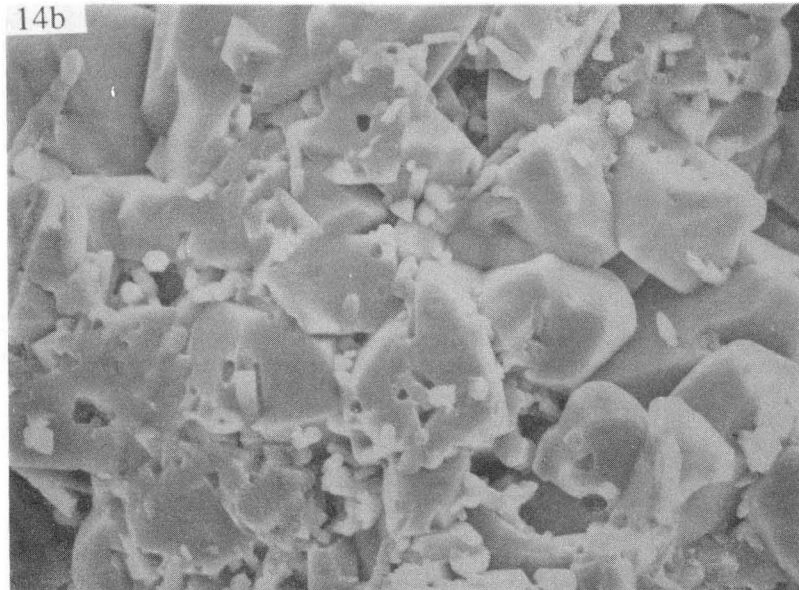
XBB904-3188

Figure 14: Fracture surfaces of 10vol% coated whisker composites.
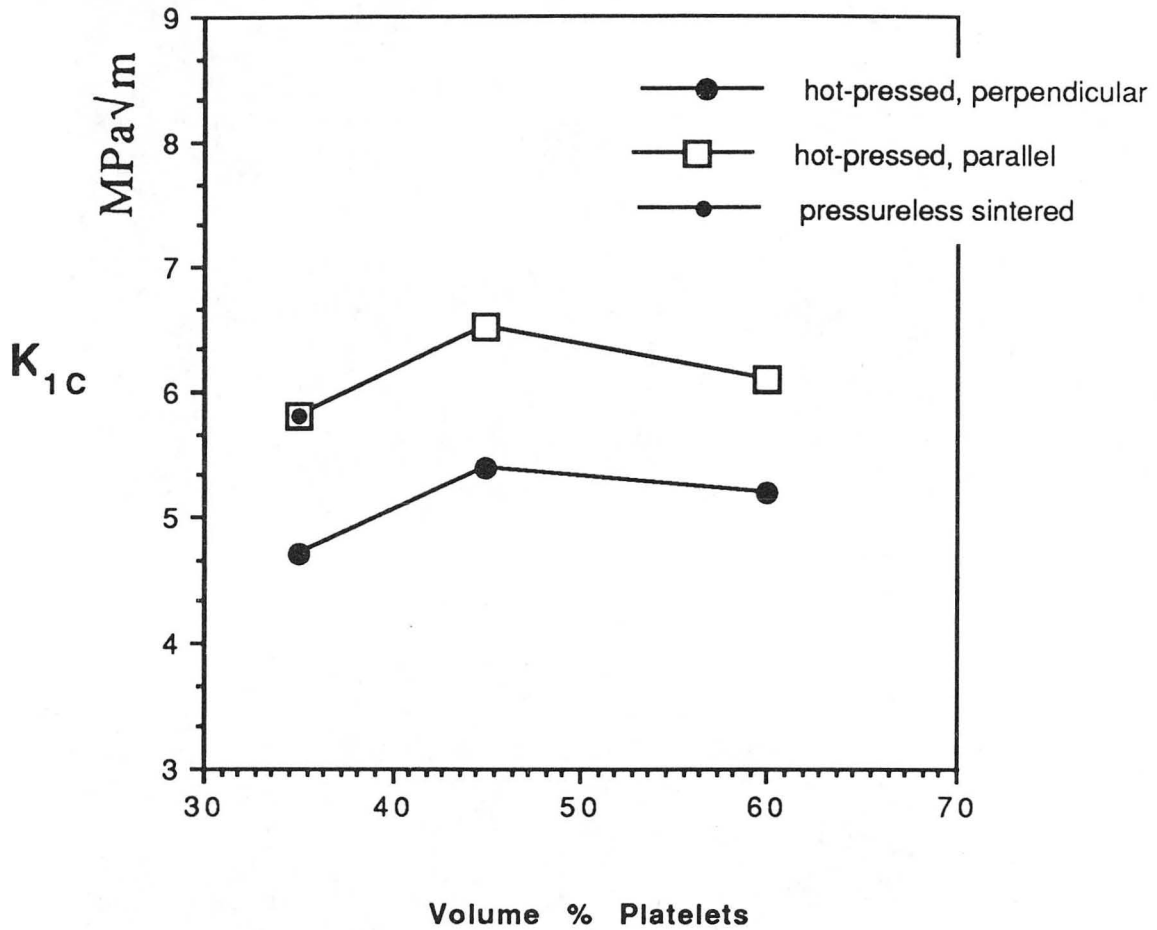(a) hot pressed (b) pressureless sintered.
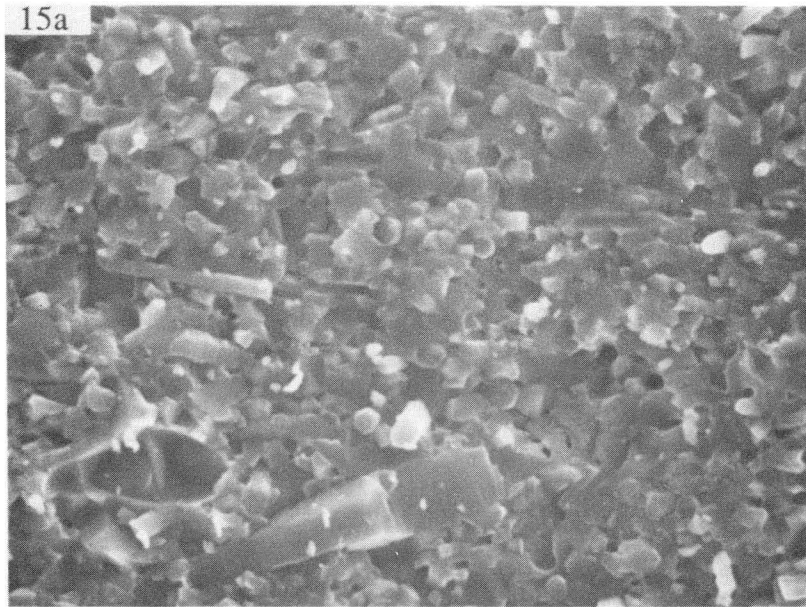
5μm
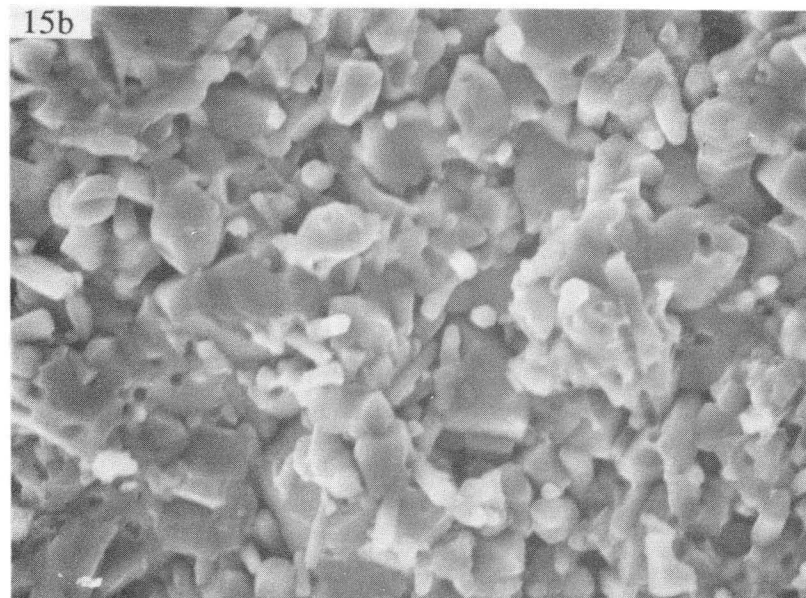
XBB904-3191

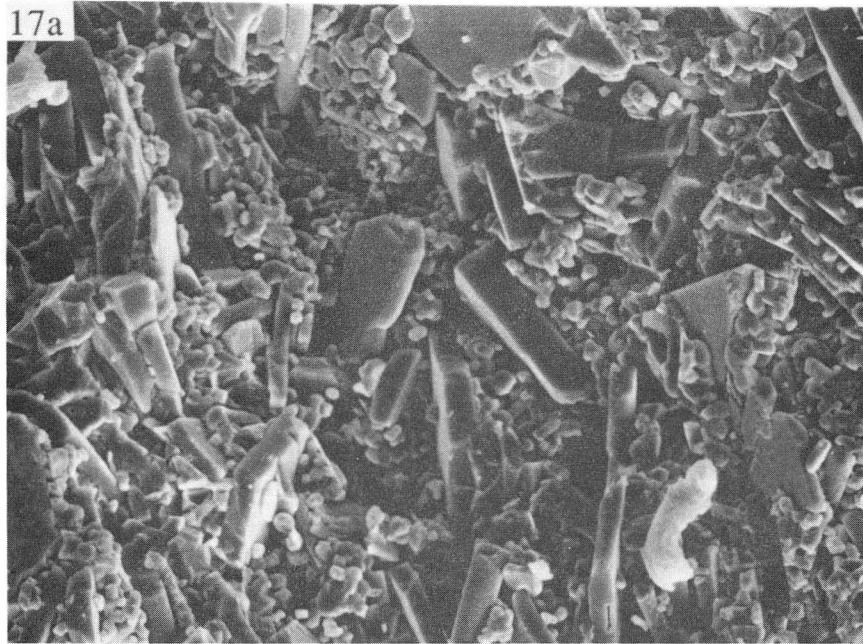Figure 15: Fracture surfaces of 25vol% coated whisker composites.
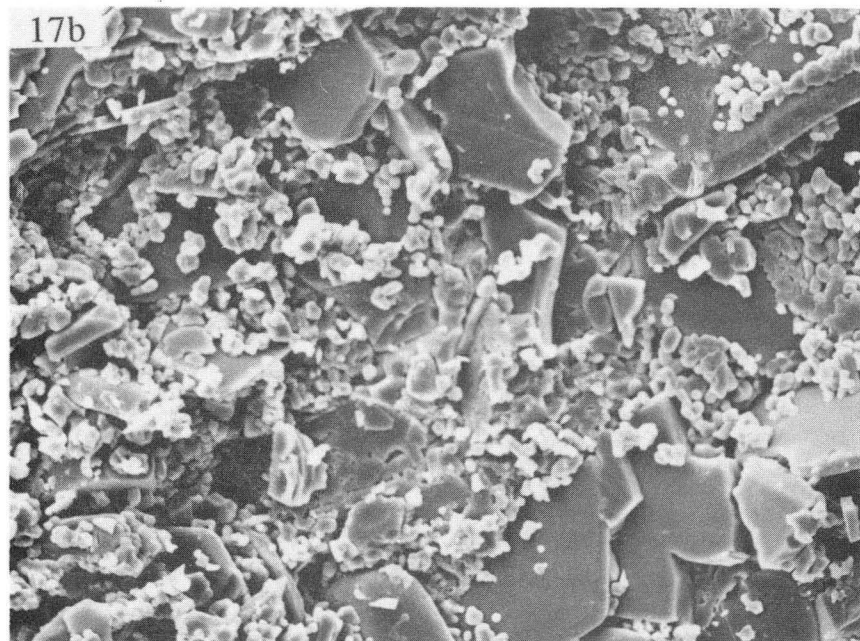(a) hot pressed (b) pressureless sintered.

50

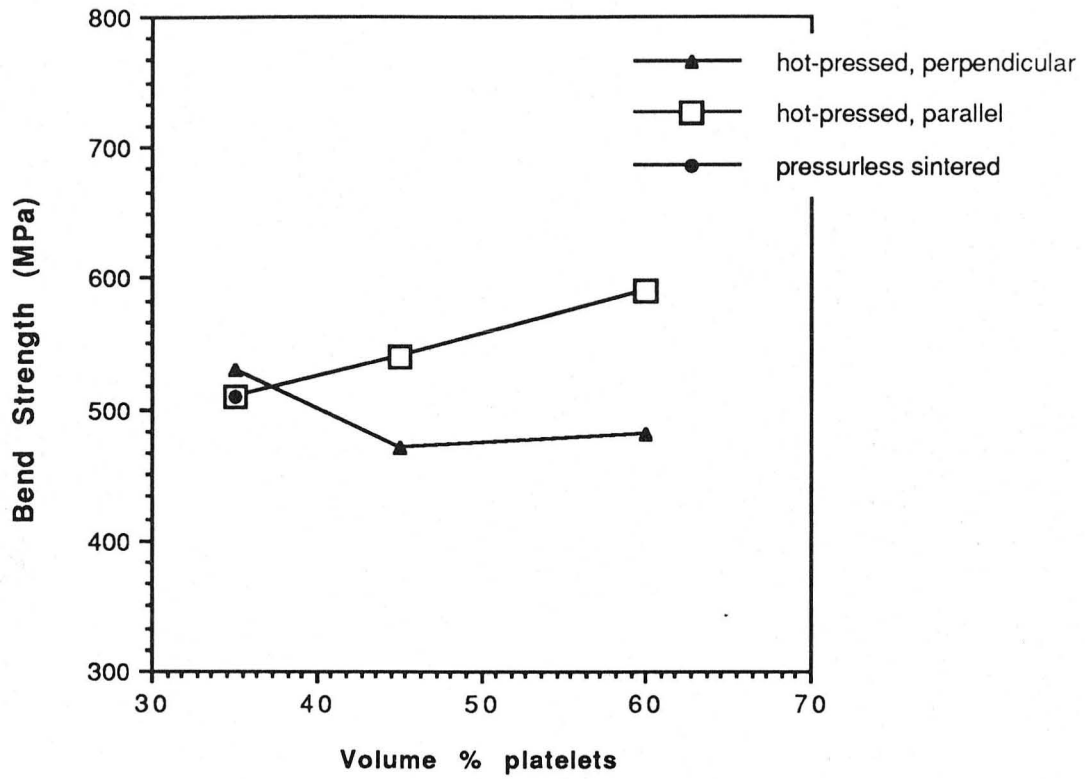Figure 16: Average fracture toughnesses of hot pressed and pressureless sintered coated platelet composites.

20μm

XBB900–10181

Figure 17: Fracture surfaces of 45vol% hot pressed coated platelet composites. (a) load applied parallel to hot pressed direction (b) load applied perpendicular to hot pressed direction.

XBL 9012-4008

Figure 18: Bend strengths of hot pressed and pressureless sintered coated platelet composites.

LAWRENCE BERKELEY LABORATORY
UNIVERSITY OF CALIFORNIA
INFORMATION RESOURCES DEPARTMENT
BERKELEY, CALIFORNIA 94720